AD-A076 214 ANALYTICAL SYSTEMS ENGINEERING CORP BURLINGTON MA F/G 20/14
LORAN-C SYSTEM DYNAMIC MODEL: TEMPORAL PROPAGATION VARIATION ST--ETC(U)
JUL 79 L W CAMPBELL , R H DOHERTY DOT-CG-829358-A
UNCLASSIFIED ASECR-79-107 USCG-D57-79 NL

1 OF 2
AD A076214

END
DATE FILMED
3-80
DDC

CONT

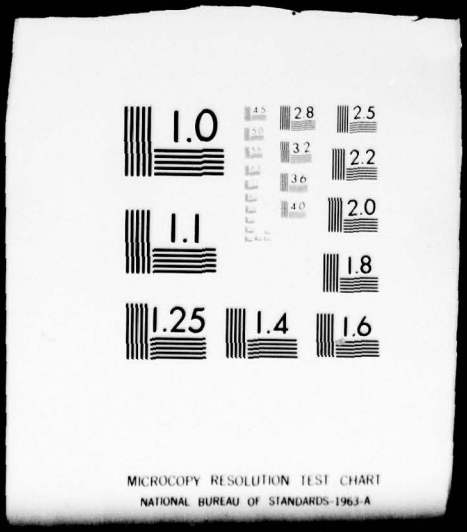

Theoretical studies as early as 1956, Reference (4), anticipated

REPORT NO. DOT-CG-D57-79

LORAN-C SYSTEM DYNAMIC MODEL
TEMPORAL PROPAGATION VARIATION STUDY

L.W. Campbell
Analytical Systems Engineering Corp.
5 Old Concord Rd.
Burlington, MA 01803

R.H. Doherty
J.R. Johler
Colorado Research and Prediction Laboratory, Inc.
1898 So. Flatiron Court
Boulder, Colorado 80301

JULY 1979
FINAL REPORT

PREPARED FOR:
U.S. DEPARTMENT OF TRANSPORTATION
UNITED STATES COAST GUARD
OFFICE OF RESEARCH AND DEVELOPMENT
WASHINGTON, D.C. 20590

NOTICE

This document is disseminated under the sponsorship of the Department of Transportation in the interest of information exchange. The United States Government assumes no liability for its contents or use thereof.

NOTICE

The United States Government does not endorse products or manufacturers. Trade or manufacturers' names appear herein solely because they are considered essential to the object of this report.

Technical Report Documentation Page

1. Report No.	2. Government Accession No.	3. Recipient's Catalog No.
DOT-CG-D57-79		

4. Title and Subtitle	5. Report Date
LORAN-C SYSTEM DYNAMIC MODEL: TEMPORAL PROPAGATION VARIATION STUDY	July 1979
	6. Performing Organization Code
	8. Performing Organization Report No.
7. Author(s) - L.W. Campbell, R. H. Doherty, J.R. Johler	ASECR 79-107

9. Performing Organization Name and Address	10. Work Unit No. (TRAIS)
ASEC 5 OLD CONCORD ROAD BURLINGTON, MA 01803 AND CRPL 1898 SO. FLATIRON BOULDER, CO 80301	11. Contract or Grant No. DOT-CG-829358-A
	13. Type of Report and Period Covered FINAL REPORT 10/1/78 - 4/30/79
12. Sponsoring Agency Name and Address U.S. DEPT. OF TRANSPORTATION UNITED STATES COAST GUARD OFFICE OF RESEARCH & DEVELOPMENT WASHINGTON, D.C. 20590	14. Sponsoring Agency Code

15. Supplementary Notes

16. Abstract

The results of a theoretical study to determine the expected extent of temporal variations in the Loran-C System are presented. Graphs of secondary phase correction vs distance, parametric in vertical lapse factor, for six values of ground impedance and parametric in ground impedance, for three values of vertical lapse factor are included. Although the secondary phase correction is most sensitive to ground impedance, it is relatively time stable and the most important parameter of concern in temporal variations is the vertical lapse factor. The effect of the surface refractive index on the secondary phase correction is negligible except in so far as it is correlated with the vertical lapse factor. A flow diagram and description of a program suitable for use on a desk calculator to calculate the secondary phase correction is included.

17. Key Words	18. Distribution Statement
LORAN-C, GROUND IMPEDANCE GROUND WAVE PROPAGATION TEMPORAL PROPAGATION VARIATIONS INDEX OF REFRACTION VERTICAL LAPSE FACTOR	DISTRIBUTION STATEMENT A Approved for public release; Distribution Unlimited

19. Security Classif. (of this report)	20. Security Classif. (of this page)	21. No. of Pages	22. Price
UNCLASSIFIED	UNCLASSIFIED		

Form DOT F 1700.7 (8-72) Reproduction of completed page authorized

METRIC CONVERSION FACTORS

Approximate Conversions to Metric Measures

Symbol	When You Know	Multiply by	To Find	Symbol
		LENGTH		
in	inches	2.5	centimeters	cm
ft	feet	30	centimeters	cm
yd	yards	0.9	meters	m
mi	miles	1.6	kilometers	km
		AREA		
in^2	square inches	6.5	square centimeters	cm^2
ft^2	square feet	0.09	square meters	m^2
yd^2	square yards	0.8	square meters	m^2
mi^2	square miles	2.6	square kilometers	km^2
	acres	0.4	hectares	ha
		MASS (weight)		
oz	ounces	28	grams	g
lb	pounds	0.45	kilograms	kg
	short tons (2000 lb)	0.9	tonnes	t
		VOLUME		
tsp	teaspoons	5	milliliters	ml
Tbsp	tablespoons	15	milliliters	ml
fl oz	fluid ounces	30	milliliters	ml
c	cups	0.24	liters	l
pt	pints	0.47	liters	l
qt	quarts	0.95	liters	l
gal	gallons	3.8	liters	l
ft^3	cubic feet	0.03	cubic meters	m^3
yd^3	cubic yards	0.76	cubic meters	m^3
		TEMPERATURE (exact)		
°F	Fahrenheit temperature	5/9 (after subtracting 32)	Celsius temperature	°C

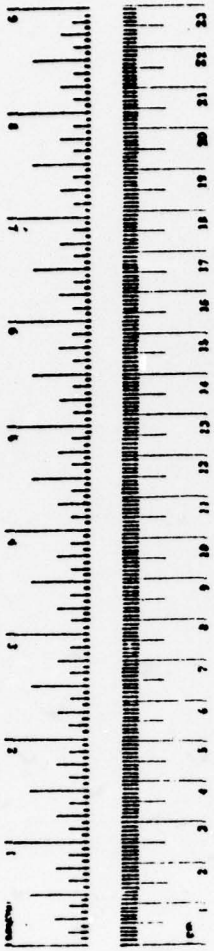

Approximate Conversions from Metric Measures

Symbol	When You Know	Multiply by	To Find	Symbol
		LENGTH		
mm	millimeters	0.04	inches	in
cm	centimeters	0.4	inches	in
m	meters	3.3	feet	ft
m	meters	1.1	yards	yd
km	kilometers	0.6	miles	mi
		AREA		
cm^2	square centimeters	0.16	square inches	in^2
m^2	square meters	1.2	square yards	yd^2
km^2	square kilometers	0.4	square miles	mi^2
ha	hectares (10,000 m^2)	2.5	acres	
		MASS (weight)		
g	grams	0.035	ounces	oz
kg	kilograms	2.2	pounds	lb
t	tonnes (1000 kg)	1.1	short tons	
		VOLUME		
ml	milliliters	0.03	fluid ounces	fl oz
l	liters	2.1	pints	pt
l	liters	1.06	quarts	qt
l	liters	0.26	gallons	gal
m^3	cubic meters	35	cubic feet	ft^3
m^3	cubic meters	1.3	cubic yards	yd^3
		TEMPERATURE (exact)		
°C	Celsius temperature	9/5 (then add 32)	Fahrenheit temperature	°F

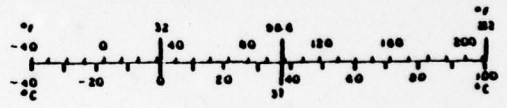

PREFACE

Extensive effort has been instituted both in the U.S. Coast Guard government efforts and in the commercial community for the further development of a comprehensive Loran-C radio navigation system. Vast areas of the northern hemisphere are now covered by Loran-C groundwave pulses from various transmitters. Receivers for position location and navigation are now available at economically reasonable prices.

Temporal variations in the propagation time of the pulses due to changes in the electrical boundary condition at the surface of the earth, or due to the atmospheric refractive index variations resulting from weather systems, interact with the propagation mechanism for the groundwave and result in degradation of the navigation accuracy for the navigator. Temporal propagation effects vary with geographic locations, climate, seasons, and perhaps on the long term correlate with the sun spot cycle. The magnitude of these effects approach the order of microseconds in anomalous geographic regions, degrading the quality of the navigation service that the transmitting system provides.

This report presents the results of a theoretical study of the possible range of temporal variations in the 100 kHz groundwave propagation mechanism. This report includes the latest state of the art developments in LF propagation as related to generalized impedance parameters and parametric evaluations of temporal variations related to meteorological parameters of the earth's atmosphere.

TABLE OF CONTENTS

TABLE OF CONTENTS (Cont.)

LIST OF FIGURES

LIST OF TABLES

1. INTRODUCTION

1.1 Loran-C Description

Loran-C is a pulsed, hyperbolic navigation system operating in the 90-110 kHz band. Ground wave range is typically 600 to 1400 nm over seawater and considerably less over land. Predictable accuracy of position information is at least 0.25 nm (2-drms) in advertised ground wave coverage areas when using automatic receivers of current design. The repeatable accuracy of the system is 60 to 300 feet (2-drms), reference (1).

Loran-C has been adopted by the U.S. Coast Guard as their standard coastal and confluence zone aid to navigation. By 1980-81, the entire U.S. Pacific and Atlantic coasts and the Gulf of Mexico will be covered, plus the Canadian Pacific Coast and the Great Lakes. The Canadian Coast Guard is considering a further Loran-C expansion over the Canadian Atlantic coast to part way up to Labrador, reference (2).

1.2 Accuracy Requirements

An accuracy of 0.25 nm (≈1500 feet) is normally adequate for navigation on the open seas and of course considerably improved accuracies are achievable as the distance between the user and the loran chain stations decreases (because of the higher signal-to-noise ratios). However, navigation in harbors and estuaries requires precise accuracy in order to navigate safely within specific channels, especially under conditions of low visibility (i.e. adverse weather conditions, nightime) and possibly a high density of traffic.

Therefore, improved accuracies in the order of 100 ft (≈100 ns) or less are required for harbor and estuary navigation. To accomplish this, error sources must be identified and their magnitudes minimized.

1.3 Sources and Magnitudes of Errors

The three basic sources of error in the Loran-C navigation system are:

- Transmitting System Synchronization errors
- Propagation errors
- Receiver measurement errors

Transmitting system errors are dependent upon the stability of the frequency standard, transmitting equipment, timing equipment, output signal phase control loops and the system area monitor/synchronization techniques. Propagation errors result from geophysical and meteorological variations along the signal path, atmospheric and man-made noise, and electromagnetic interference. Receiver measurement errors are dependent upon receiving equipment performance, antenna environment, relative motion, and system geometry (GDOP).

To provide increased navigation accuracy, these error sources must be minimized. In doing this, the three modes of operation of a Loran-C chain should be considered. These are:

1. The repeatable modes, i.e., ability of navigator to return to the same loran coordinates again and again.
2. The predictability mode, or the ability of the navigator to give his geographic coordinates with precision, using the loran coordinates.
3. The relative or differential loran mode, or the ability of the navigator to locate position relative to a known position using loran.

Inaccuracies introduced into the system due to transmitting system synchronization errors are within $\pm$ 50 nanoseconds, which is the control tolerance for timing adjustments at the secondary stations.

Receiver measurement errors can be minimized by using quality equipment, proper equipment configuration and operation, and optimum crossing angles of the hyperbolic lines-of-position. A theoretical error budget for the INTERNAV-LC204 hard limiting receiver utilizing 100-second averaging has been reported by GE-TEMPO, reference (3), to be of the order of 10-17 nanoseconds. Values of 30-60 nanoseconds error for a typical commercial receiver using 5-second averaging are also reported, reference (3).

In contrast to errors of the order of say 50-100 nanoseconds for the transmitting system synchronization and the receiver measurements, propagation errors are significantly higher, i.e. 400-3000 nanoseconds.

Propagation errors occur in general because the Loran-C signal velocity varies with position. The signal is slowed down by the physical and electrical properties of the earth's/air surface interface. These include the impedance or conductivity of the ground, the roughness or terrain varations of the surface, the refractive index of the atmosphere at the surface, and the lapse rate or (rate of change of refractive index with height above the surface).

Spatial (geophysical) variations, of the transmitted signals are primarily influenced by the inhomogeneities of the surface impedance and the variations in the terrain. Temporal (meteorological) effects are produced by time changes in these spatial features, and are also influenced by the surface refractive index and the lapse rate of the refractive index of the earth's atmosphere, (which are known to change diurnally and with changing weather conditions).

The spatial propagation error dominates all other errors. However, it is time stable and its effects can be accommodated through grid calibration programs. Methods involving time difference measurements have been used to warp the Loran-C hyperbolic grid lines to cancel out these fixed spatial dependent errors.

Temporal related propagation effects, although of smaller magnitude, create a more difficult problem for maintaining the most stable grid.

Theoretical studies as early as 1956, Reference (4), anticipated the existence of temporal changes in the phase of the Loran-C signal as a result of natural changes with time in the propagation mechanism of the ground wave. Fortunately the ground wave exhibits a remarkable stability with time. Without such stability, Loran-C precision navigation would not be possible. However, as the loran technical community strives for ever greater accuracy and precision, the small but measurable temporal variations in the ground wave propagation mechanism become more and more important. With a total allowable budget error in the order of 100 nanoseconds, temporal errors should be minimized to about 10 nanoseconds for the combination of propagation, transmitter, and receiver system errors to approach 100 nanoseconds.

2. OBJECTIVE

2.1 Characterization of Temporal Propagation Variations

The primary objective of this program is to characterize temporal propagation variations in terms of secondary phase corrections as a function of distance for varying conditions related to meteorological changes. The variable parameters to be considered include the surface refractive index, the vertical lapse factor, and the electrical characteristics of the ground.

Although terrain effect is very important, its effect will not be considered here directly. Generally, irregularities in terrain increase the effective ground surface impedance, x. Therefore, to correctly interpret results presented here, the electrical characteristics of the ground mentioned above should be taken as the effective surface impedance which includes terrain effects.

2.2 Assessment of Impact on Loran-C Chain Control

A secondary objective of this program is to assess the impact of using knowledge of temporal propagation variations to improve Loran-C Chain Control. System Area Monitors (SAMs) are used to insure the maintenance of the emission delay at the secondary transmitters as a chain constant. This imposes problems connected with sorting out system timing synchronization changes over the baselines and propagation changes over the paths to the monitor. The system timing changes over the baselines have been obviated by the use of the cesium oscillator clocks but system changes at the monitor still reflect both system timing and propagation changes with time. Since propagation changes are not linearly distributed in space and time, the removal of any gross system changes through the dictates of the area monitor automatically tends to remove the nonlinear propagation temporal changes at the monitor. However, propagation temporal changes removed at the monitor geographic location will not be appropriate for some other point. It is therefore important that propagation effects in the time domain (temporal effects) be taken into account in both space and time dimensions as the chain management strives for ever greater Loran-C accuracy and precision.

3. ANALYSIS

3.1 Definition of Variables and Causal Mechanisms

The causes of ground wave temporal changes that can be identified in the existent theory of propagation of the ground wave are (not necessarily in order of importance), reference (5):

(1) The surface impedance of the ground variations with climate and weather;

(2) The index of refraction of air variations at the surface of the ground with weather, climate and ground elevation;

(3) The variations of the gradient of the index of refraction at the surface of the ground with altitude above the surface of ground (vertical lapse of refractive index); and

(4) The more subtle effects of terrain roughness, elevation, soil consistency, geologic underlayment, as it interacts with weather and climate to produce both ground impedance changes and atmospheric changes such as temperature inversions.

It should be noted that temporal effects can be diurnal, seasonal and perhaps even exhibit long term effects correlated with the sunspot cycle.

3.2 Establishment of Variables Base

3.2.1 Surface Index of Refraction (η_a)

The index of refraction of air at the surface of the ground grossly affects the primary wave propagation time and is usually designated by the constant value $\eta_a = 1.000338$. This is an average value

given in reference (6) and it is certainly not a constant either geographically or temporally. Actually η_a may vary between 1.0002 and 1.0004 or, reference (5), between 200 and 400 N-units where,

$$N = (\eta_a - 1)\ 10^6$$

Studies, reference (5), show that the secondary phase correction is substantially independent of the surface refractive index. However there is a strong correlation between the surface refractive index and the vertical lapse factor, α, and α strongly affects the secondary phase correction.

3.2.2 Vertical Lapse Factor (α)

Changes in surface temperature and indeed surface N-factor have been correlated strongly with the vertical lapse factor. Since the vertical lapse factor, which shall be designated as α, enters into the ground wave theory as a parameter, calculations of the ground wave parametric in α can be used to estimate the effects of climate and weather that are observed at the surface of the ground. Of course, if information on N-units aloft are available, these also can be used to deduce the α factor.

The temporal variations associated with weather changes at the surface of the ground have been clearly identified in a number of papers, References (7, 8, 9, 10 11 and 12). Although strongly correlated with the surface value of index of refraction $\eta(h)$, $h = 0$, these variations can only be explained by the atmospheric vertical lapse variations in the index of refraction, $\eta(h)$, where h is the altitude above the surface.

For Loran-C, α may vary from about 0.6 to 1.2 and the atmosphere $\eta(h)$ is not necessarily exponential.

3.2.3 Ground Electrical Characteristics (x)

The secondary phase correction is also a function of the electrical characteristics of the ground. These ground characteristics can be expressed as a complex number x which is a normalized surface impedance. If an effective value of x is used or if the ground is homogeneous, the classical ground wave theory permits calculation of the secondary phase correction. Typical values of x are given in Table 1 and Table 2, reference (5).

The values of amplitude $|x|$ and phase, Arg(x), given in Table 1 define the region of the complex plane that has been found through ob servations to be most appropriate to Loran-C. These values give the part of the complex x-plane that has been used in practice to represent the ground surface impedance throughout the world for various Loran-C chains. These values cover a range of effective values that are physically realizable. In contrast, ground effective conductivity (σ) values given in Table 2 may or may not be physically realizable. The most common value, σ = 5 mhos/m, is valid over sea water and corresponds to an impedance of .001055 exp (j .78535). On the other hand, the values near σ = 0.0001 mhos/m are not realized at Loran-C frequencies because waves penetrating the ground as the conductivity decreases are reflected at various levels and the phase of the complex impedance (x) moves away from $\pi/4$ (for sea water) to typically inductive values of impedance near 1 radian.

3.3 Secondary Phase Correction Calculations

The phase of a Loran-C ground wave signal is usually expressed as

$$\phi = \frac{\omega}{c} \eta_a d + \phi_c$$

TABLE 1

RELATIONSHIP BETWEEN IMPEDANCE
MODULUS, $|x|$, and ARGUMENT, $\mathrm{Arg}(x)$, $h = 0$

$\lvert x\rvert$	$\mathrm{Arg}\,(x)$	$\lvert x\rvert$	$\mathrm{Arg}\,(x)$
.001	.7854	.04182	.8198
.0010549	.78535	.043038	.8268
.002	.7845	.044305	.8339
.003	.7837	.045	.8377
.004	.7830	.050	.8635
.005	.7823	.055	.8885
.006	.7816	.060	.9150
.007	.7809	.08	1.036
.008	.7802		
.009	.7795		
.010	.7788		
.011	.7781		
.012	.7774		
.013	.7767		
.014	.7760		
.015	.7753		
.016	.7745		
.017	.7738		
.018	.7731		
.019	.7724		
.020	.7717		
.021	.7710		
.022	.7702		
.023	.7694		
.024	.7687		
.025	.7679		
.025473	.7672		
.026979	.7658		
.02719	.7658		
.027648	.7658		
.027793	.7657		
.028	.7655		
.029	.7663		
.030	.7678		
.031	.7700		
.032	.7730		
.033	.7762		
.034	.7800		
.035	.7845		
.036	.7890		
.037	.7945		
.038	.7995		
.039	.8055		
.040	.8115		
.04008	.8116		
.041206	.8163		

TABLE 2

RELATIONSHIP BETWEEN CONDUCTIVITY (σ) AND HOMOGENEOUS GROUND IMPEDANCE WITHOUT IRREGULARITIES OR NON-HOMOGENEITIES

σ, mhos/m	$\lvert x \rvert_{i,k}$	Arg $(x)_{i,k}$	ϵ_2
.0001	.20395	.42082	15
.0002	.15950	.57579	15
.0003	.13340	.64109	15
.0004	.11657	.67588	15
.0005	.10470	.69729	15
.0006	.09581	.71174	15
.0007	.08882	.72215	15
.0008	.08316	.72999	15
.0009	.07846	.73610	15
.0010	.07447	.74100	15
.0020	.05273	.76316	15
.0030	.04307	.77057	15
.0040	.03730	.77427	15
.0050	.03337	.77650	15
.0060	.03046	.77798	15
.0070	.02820	.77904	15
.0080	.02638	.77983	15
.0090	.02487	.78045	15
.0100	.02359	.78095	15
.0200	.01668	.78317	15
.0300	.01362	.78391	15
.0400	.01180	.78429	15
.0500	.01055	.78451	15
.0600	.00963	.78466	15
.0700	.00892	.78476	15
.0800	.00834	.78484	15
.0900	.00786	.78490	15
.1000	.00746	.78495	15
.2000	.00528	.78518	15
.3000	.00431	.78525	15
.4000	.00373	.78529	15
.5000	.00334	.78531	15
.6000	.00305	.78532	15
.7000	.00282	.78533	15
.8000	.00264	.78534	15
.9000	.00249	.78535	15
1.	.00236	.78535	15
2.	.00167	.78538	15
3.	.00136	.78538	15
4.	.00118	.78539	15
5.	.00106	.78539	15
5.	.00106	.78535	80

where $\omega = 2\pi f$; (f being the signal frequency in Hertz)

η_a = refractive index of air at ground level

c = velocity of light in vacuum

d = transmitter to receiver separation distance

ϕ_c = secondary phase correction, caused by finite impedance and refractive index discontinuities across the boundary along which the signal propagates.

Secondary phase correction can be expressed as:

$$\phi_c \approx (ak_1)^{1/3} \alpha^{2/3} \tau_o \left(\frac{d}{a}\right) \text{ radians} \qquad (1)$$

or $t_c = (\phi_c/\omega)\, 10^6$ Microseconds

where

a = earth radius

k_1 = wave number = $\left(\frac{\omega}{c}\right)\eta_a$

$\tau_o \rightarrow$ is primarily influenced by surface impedance and is derived from the boundary condition at the surface of the ground as the zero'th root of a Riccati differential equation and at 100 kHz is typically ≈0.42

$\alpha \rightarrow$ is associated with the lapse rate of the refractive index. The formula relating α to the change of η with height is

$$\alpha = 1 + \frac{a}{\eta_a} \frac{\left[\frac{d\ \eta\ (a + h)}{d\quad (a + h)}\right]}{} \qquad (2)$$

Equation (2) has an alternate representation in terms of measurable atmospheric variables.

$$\alpha = 1 - \left(\frac{a}{h_b}\right)\left(1 - \frac{1}{\eta_a}\right)\left(1 - \frac{N_b}{N_a}\right) \qquad (3)$$

where

$N_a = (\eta_a - 1)\ 10^6$

$N_b = (\eta_{h_b} - 1)\ 10^6$

h_b is altitude above the surface

The N-units at any height can be written:

$$N = (\eta - 1)10^6 = \frac{77.6}{T}\left[P + \frac{4810e}{T}\right] \qquad (4)$$

together with the hydrostatic equation:

$$\frac{dP}{dh} + \frac{de}{dh} = -10g\rho \qquad (5)$$

where

h is in meters
g = the gravitational constant (cm sec^{-2}),
ρ = density of air (grams cm^{-3}),
P = atmospheric pressure [millibars] (kg $cm^{-1}sec^{-2}$),
T = temperature [°Kelvin],
e = partial pressure of water vapor [millibars], (kg $cm^{-1}sec^{-2}$).

The 10 is necessary to make the equation dimensionally correct and dimensionally relative to equation 4.

Then,

$$\frac{dN}{dh} = -\left\{\frac{776 \times 1.268}{T} + \frac{77.6}{T^2}\left[P + \frac{9620e}{T}\right]\frac{dT}{dh}\right.$$

$$\left. + \frac{77.6}{T}\left[1 - \frac{4810}{T}\right]\frac{de}{dh}\right\} \qquad (6)$$

and

$$\alpha = 1 + \frac{a}{\eta}\frac{d\eta}{dh} \qquad (7)$$

where $a/\eta \sim a$ and $a = 6.378(10^6)$ meters, (Reference 15.)

α is evaluated at various temperatures using a unit height of 100 meters and P equal to 1013.25 mb. Thus,

at -15°C $\quad \alpha = .756 - \left\{.0753 + .00277e\right\} \frac{dT}{dh} + .358 \frac{de}{dh}$

at 0°C $\quad \alpha = .770 - \left\{.0673 + .00234e\right\} \frac{dT}{dh} + .301 \frac{de}{dh}$

at 27°C $\quad \alpha = .791 - \left\{.0557 + .00176e\right\} \frac{dT}{dh} + .264 \frac{de}{dh}$

at 35°C $\quad \alpha = .796 - \left\{.0529 + .00163e\right\} \frac{dT}{dh} + .251 \frac{de}{dh}$

Also for homogeneous atmosphere*, $de/dh = - mg/RT\ e$ (Reference 16)

at -15°C $\frac{de}{dh} = -.0132e/100$ m

at 0°C $\frac{de}{dh} = -.0125e/100$ m

at 27°C $\frac{de}{dh} = -.0113e/100$ m

at 35°C $\frac{de}{dh} = -.0111e/100$ m

The temperature lapse rate would be expected to be between the adiabatic lapse rate of -.98°C/100 m and the dew point lapse of - 17°C/100m. Reference 16 gives a derivation of the temperature lapse rate in a homogeneous atmosphere and indicates that for a mixing ratio of 10 mille which corresponds to 16 mb of vapor pressure the temperature lapse rate would be one-half the dry adiabatic value. Therefore, for purposes of evaluating α values, two average temperature lapse rates have been assumed that are: -.98°C/100 m and -.49°C/100 m.

*Meteorological explanation of homogeneous atmosphere.

Over land paths the diurnal temperature will vary considerably due to the solar heating and nocturnal cooling of the earth's surface. The extremes of the temperature variations are therefore assumed to reach from $-4^{\circ}C/100$ m at noon to $+4^{\circ}C/100$ m at midnight. These extremes represent a 8.16 or 4.08 multiplicative factor from the -.49 or $-.98^{\circ}C/100$ m lapse rates. The water vapor lapse rate will change proportionally with the temperature lapse rate. Therefore the same multiplicative factors are applied to the de/dh lapse rate as are applied to th dT/dh lapse rate in an attempt to derive α values for winter and summer conditons from the formulas given in the previous section.

For Winter Conditions

Moderate Winter $0^{\circ}C$, 50% humidity, i.e. e = 3 mb, $\frac{de}{dh}$ = -.0375 mb/100 m

	dT/dh		de/dh
Average Conditions	$-.98^{\circ}C/100$ m	and	-.0375 mb/100 m
(Homogeneous Atmosphere)	$-.49^{\circ}C/100$ m	and	-.0375 mb/100 m
Extreme for Noon	$-4^{\circ}C/100$ m	and	-.153 mb/100 m
	$-4^{\circ}C/100$ m	and	-.306 mb/100 m
Extreme for Midnight	$+4^{\circ}C/100$ m	and	+.153 mb/100 m
	$+4^{\circ}C/100$ m	and	+.306 mb/100 m

Extreme Winter - 15° C, 50% Humidity i.e. e = 1 mb, $\frac{de}{dh}$ -.0132 mb/100 m

	dT/dh		de/dh
Average Conditions	$-.98^{\circ}C/100$ m	and	-.0132 mb/100 m
(Homogeneous Atmosphere)	$-.49^{\circ}C/100$ m	and	-.0132 mb/100 m
Extreme for Noon	$-4^{\circ}C/100$ m	and	-.0539 mb/100 m
	$-4^{\circ}C/100$ m	and	-.108 mb//100 m
Extreme for Midnight	$+4^{\circ}C/100$ m	and	+.0539 mb/100 m
	$+4^{\circ}C/100$ m	and	+.108 mb/100 m

For Summer Conditions

Moderate Summer 27°C, 50% Humidity, i.e. e = 17.5 mb, $\frac{de}{dh}$ = -.198 mb/100 m

	dT/dh		de/dh
Average Conditions	-.98°C/100 m	and	- .198 mb/100 m
(Homogeneous Atmosphere)	-.49°C/100 m	and	- .198 mb/100 m
Extreme for Noon	-4°C/100 m	and	- .808 mb/100 m
	-4°C/100 m	and	-1.62 mb/100 m
Extreme for Midnight	+4°C/100 m	and	+ .808 mb/100 m
	+4°C/100 m	and	+1.62 mb/100 m

Extreme Summer 35°C, High Humidity, and e = 42 mb, $\frac{de}{dh}$ = -.466mb/100 m

	dT/dh		de/dh
Average Conditions	-.98°C/100 m	and	-.466 mb/100 m
(Homogeneous Atmosphere)	-.49°C/100 m	and	-.466 mb/100 m
Extreme Noon	-4°C/100 m	and	-1.90 mb/100 m
	-4°C/100 m	and	-3.80 mb/100 m
Extreme Midnight	+4°C/100 m	and	+1.90 mb/100 m
	+4°C/100 m	and	+3.80 mb/100 m

Calculated α values are given below in Table 3. These can be interpreted as follows:

Winter conditions yield inverse correlation between propagation velocity and temperature as discussed extensively in Reference 8. That is, the lower the temperature the faster the signal travels or the smaller the phase delay for a given path. During summer conditions a negative term associated with dT/dh and a positive term associated with de/dh tend to cancel each other. During average or normal summer conditions these factors tend to offset keeping the alpha value between approximately .75 and .85. Also, under extreme summer conditions a correlation with temperature can average all the way from the winter time inverse correlation to a high temperature summer time direct correlation shown for +35°C and dT/dh = -.49°C/100 m in Table 3.

TABLE 3

α Values Calculated for Various Conditions Listed Above

	dT/dh = -.49	dT/dh = -.98
Moderate Winter Conditions are T = 0°C		
Average	α = .795	α = .832
Extreme Noon	α = .975	α = 1.02
Extreme Midnight	α = .565	α = .519
Extreme Winter Conditions are T = -15°C		
Average	α = .790	α = .828
Extreme Noon	α = 1.03	α = 1.05
Extreme Midnight	α = .482	α = .463
Moderate Summer Conditions are T = 27°C		
Average	α = .781	α = .823
Extreme Noon	α = .709	α = .924
Extreme Midnight	α = .873	α = .658
Extreme Summer Conditions are T = 35°C		
Average	α = .738	α = .798
Extreme Noon	α = .328	α = .804
Extreme Midnight	α = 1.26	α = .787

Finally, these results suggest that Loran-C temporal variations both in the summer and in the winter should be directly predictable from surface measurements. The temperature and humidity lapse rates dT/dh and de/dh will be determined by the surface values of the temperature and humidity along with the history of their variations as observed and recorded in the immediate past. An experimental program to prove this should be initiated.

Another example derived from Reference 16 is shown in Figure 1. The information in Figure 1 and in Table 3 tends to show the same results. Figure 1 shows that when de/dh in mb/100 m is equal to .4 x dT/dh in ^{o}C/100 m, the changes in the lapse rate dN/dh will tend to cancel. For winter conditions where de/dh = -.0132 mb/100 m to -.0375 mb/100 m and dT/dh = -.49^{o}C/100 m to -.98^{o}C/100 m, the condition for equilibrium is not met, whereas in the summer when de/dh = -.198 mb/100 m to -.466 mb/100 m and the dT/dh = -.49^{o}C/100 m to -.98^{o}C/100 m, the condition for equilibrium is met and actually reversed.

All of this material then tends to support theoretical predictions of Loran-C temporal effects. It supports the observed large winter temporal variations and small summer temporal variations that have been consistently observed on the U.S. East Coast path between Dana, Indiana and Carolina Beach, N.C. An experiment utilizing Loran-C measurements and surface meteorlogical measurements over paths subject to extreme summer and winter conditions should establish this relationship through data analysis techniques.

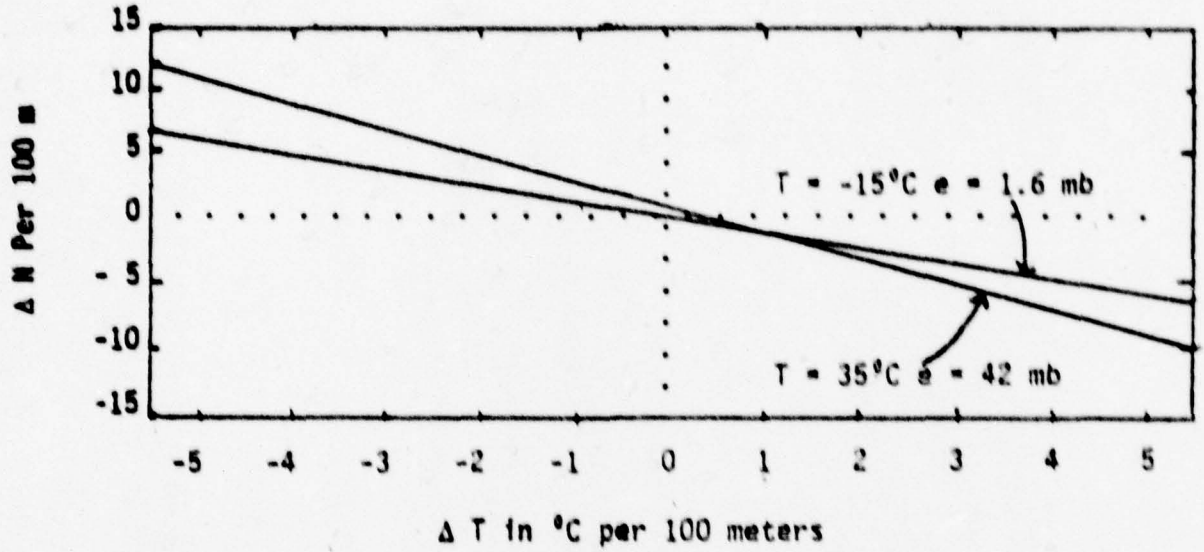

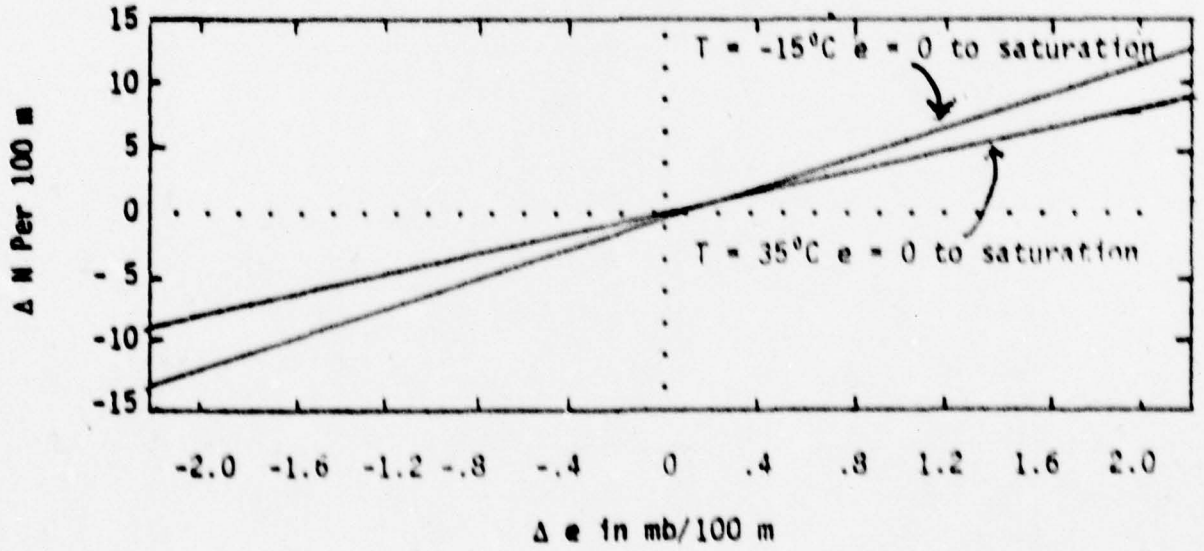

Figure 1 Illustrating ΔN as a Function of Δe and ΔT at Select Values of Temperature, T.

4. ANALYTICAL RESULTS

4.1 Atmospheric Temporal Effects

Atmospheric temporal variations are correlated with surface refractive index and the vertical lapse rate of the surface refractive index. The phase temporal variations that are caused by change in η_a, the surface refractive index, are caused by changes in the primary wave. The primary wave phase, ϕ, is,

$$\phi = \frac{\omega}{c} \eta_a d, \tag{6}$$

and the phase changes associated with the surface refractive index is simply

$$\Delta \eta_a \cdot d,$$

which quantity is in microseconds if d is in kilometers. Therefore, a change from

$$\eta_a = 1.0002 \text{ to } 1.0004,$$

(the maximum η_a variation) over a propagation path with a length of 1000 km would yield a phase change of 0.2 microseconds. Normally the change in average value ($\eta_a = 1.000338$) over a day or during a weather change would be only 40 N-units (N-units = $(\eta_a - 1)\ 10^6$). Therefore, the maximum diurnal or weather change effect that could be attributed to changes in η_a for a 1000 km propagation path would be 0.04 microseconds, or 40 nanoseconds. This amount of variation may be nearly typical of the variations observed over a 1000 km propagation path during warm weather. However, in cold weather, the observed variations are typically an order of magnitude or more greater than this value, reference (8). As a result the overall winter weather variations observed over an approximately 1000 km propagation path have been attributed to changes in the vertical lapse factor.

4.1.1 Graphs Depicting Atmospheric Temporal Effects

Graphs of secondary phase correction (t_c) vs distance, parametric in vertical lapse factor (α), for select values of ground surface impedance x (or conductivity σ) are given in Figures 2 through 7. Since there is a negligible effect due to changes in the surface refractive index (η_a) except in so far as η_a is correlated with α, these curves hold, for all values of η_a from 1.0002 to 1.0004. α values range from 0.65 to 1.20 for each graph.

Figures 2 and 3 are very similar. The former is based on a seawater ground impedance x = .0011 (σ = 4.6 mhos/m) taken from Table 1 in Section 3 and the latter is based on seawater ground impedance $|x|$ = .001055 (σ = 5.0 mhos/m) taken from Table 2 in Section 3. Although not perceptable on the graphs, a change in the secondary phase correction of the order of nanoseconds is produced. Furthermore, a comparison of the values of the secondary phase correction using seawater ground impedance with the values in Figures 4 through 7 demomstrates the strong dependence of the secondary phase correction on the ground surface impedance. Values of t_c at 1600 km over seawater (Figure 2 and 3) are of the order of 2.5 to 4.0 μs whereas for poor earth (Figure 7) they are 13 to 17 μs.

These graphs clearly show the importance of α in temporal propagation changes. The change in t_c between the extreme values of α is $\sim$1.5μs for seawater (Figure 2) and $\sim$4.5 μs for poor earth (Figure 7) at a distance of 1600 km. It should be pointed out that the phase correction change $\Delta(t_c)$ is proportional to a $\Delta(\alpha^{2/3})$ and a Δd, where d is distance. Since $\Delta(\alpha^{2/3})$ is smaller than Δd the effect of $\Delta(\alpha^{2/3})$ on $\Delta(t_c)$ is more evident at greater distances. An expanded graph is given in Figure 8 to more clearly illustrate the effects of α at short distances. This shows that Δt_c is about 0.1μs at 200 km for a change in α from 0.65 to 1.0 over average ground.

4.1.2 Relationship of α Values With Observations.

The seasonal, diurnal and other temporal variations observed over the 1000 km propagation path between Dana, Indiana and Carolina Beach,

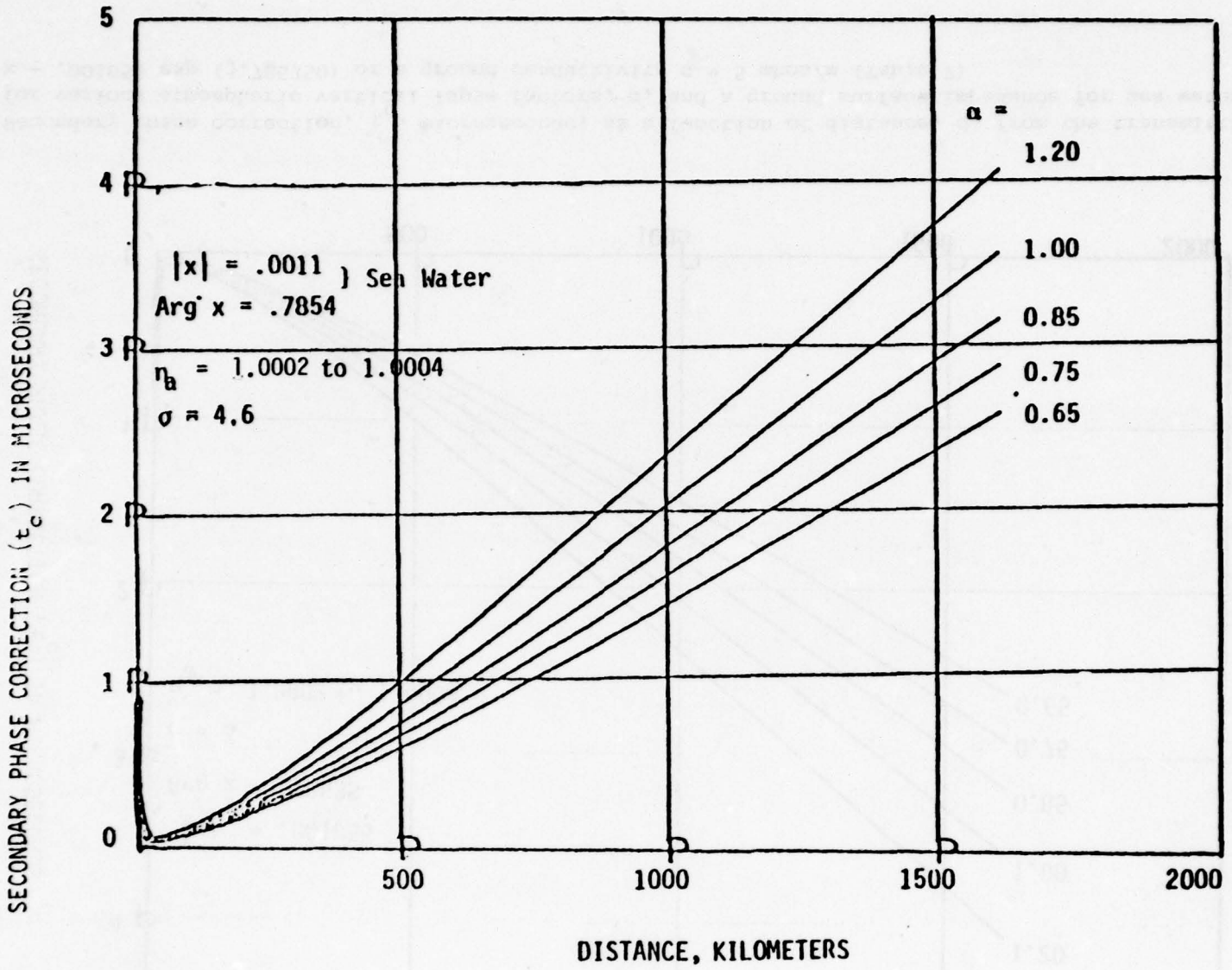

Figure 2 Secondary phase correction, t_c, microseconds, as a function of distance, d, from the transmitter for various atmospheric vertical lapse factors, α, and a ground surface impedance for sea water x = .0011 exp (j,7854) or a conductivity σ = 4.6 mhos/m (Table 2).

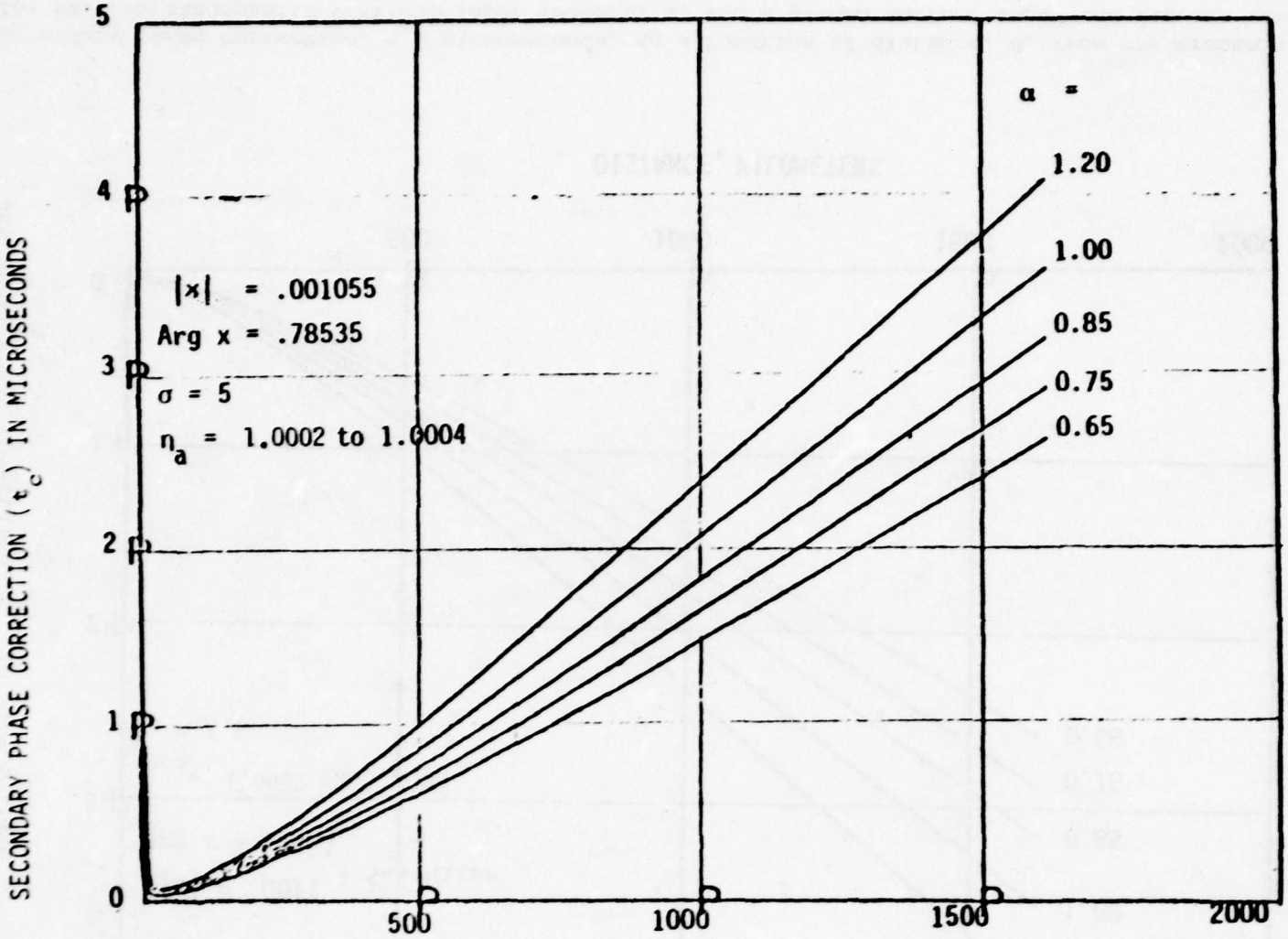

Figure 3 Secondary phase correction, t_c, microseconds, as a function of distance, d, from the transmitter for various atmospheric vertical lapse factors, α, and a ground surface impedance for sea water x - .001055 exp (j.785350) or a ground conductivity σ = 5 mhos/m (Table 2)

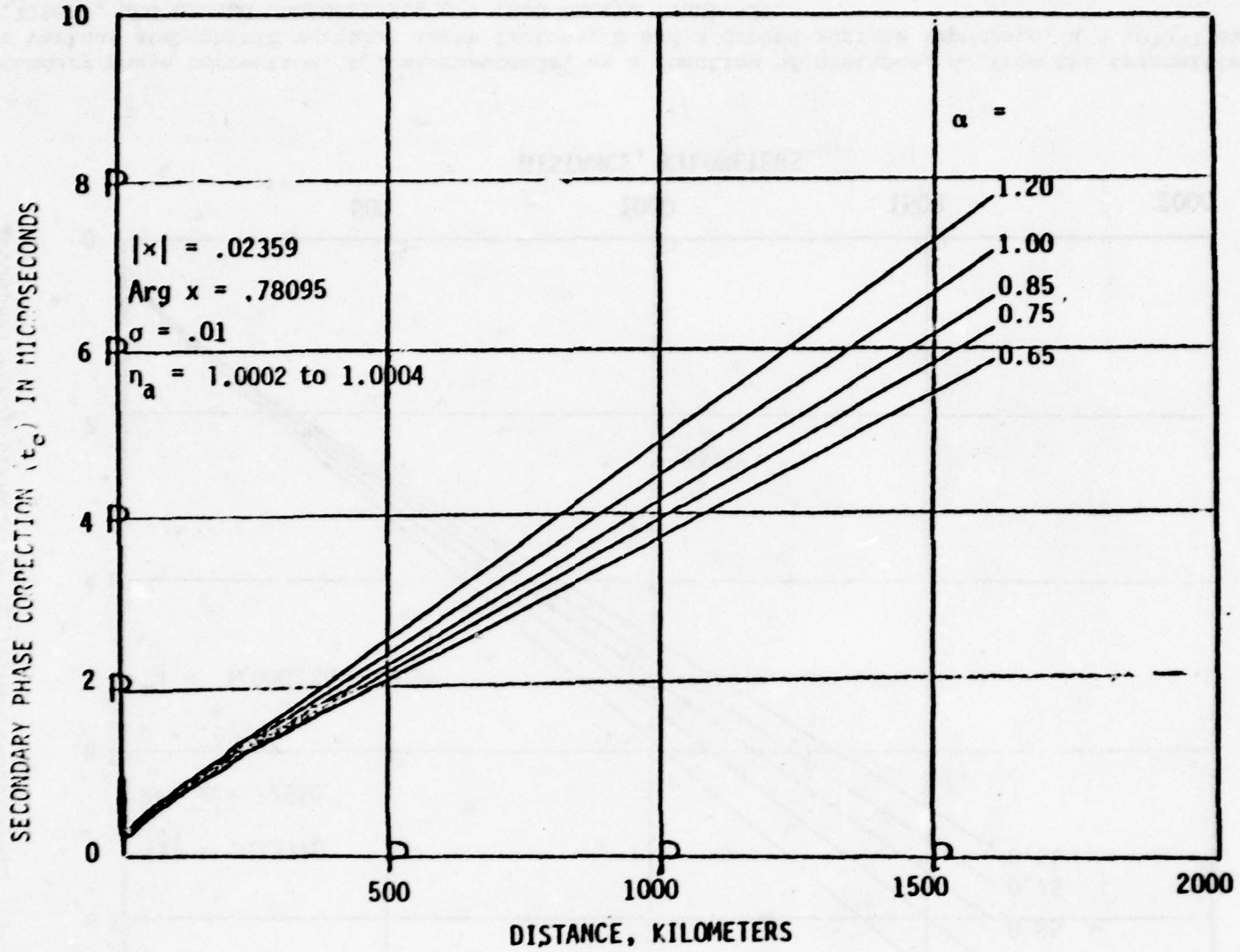

Figure 4 Secondary phase correction, t_c, microseconds, as a function of distance, d, from the transmitter for various atmospheric vertical lapse factors, α, and a ground surface impedance, x = 02359 exp (j .78095), or a ground conductivity σ = .01 mhos/m (Table 2).

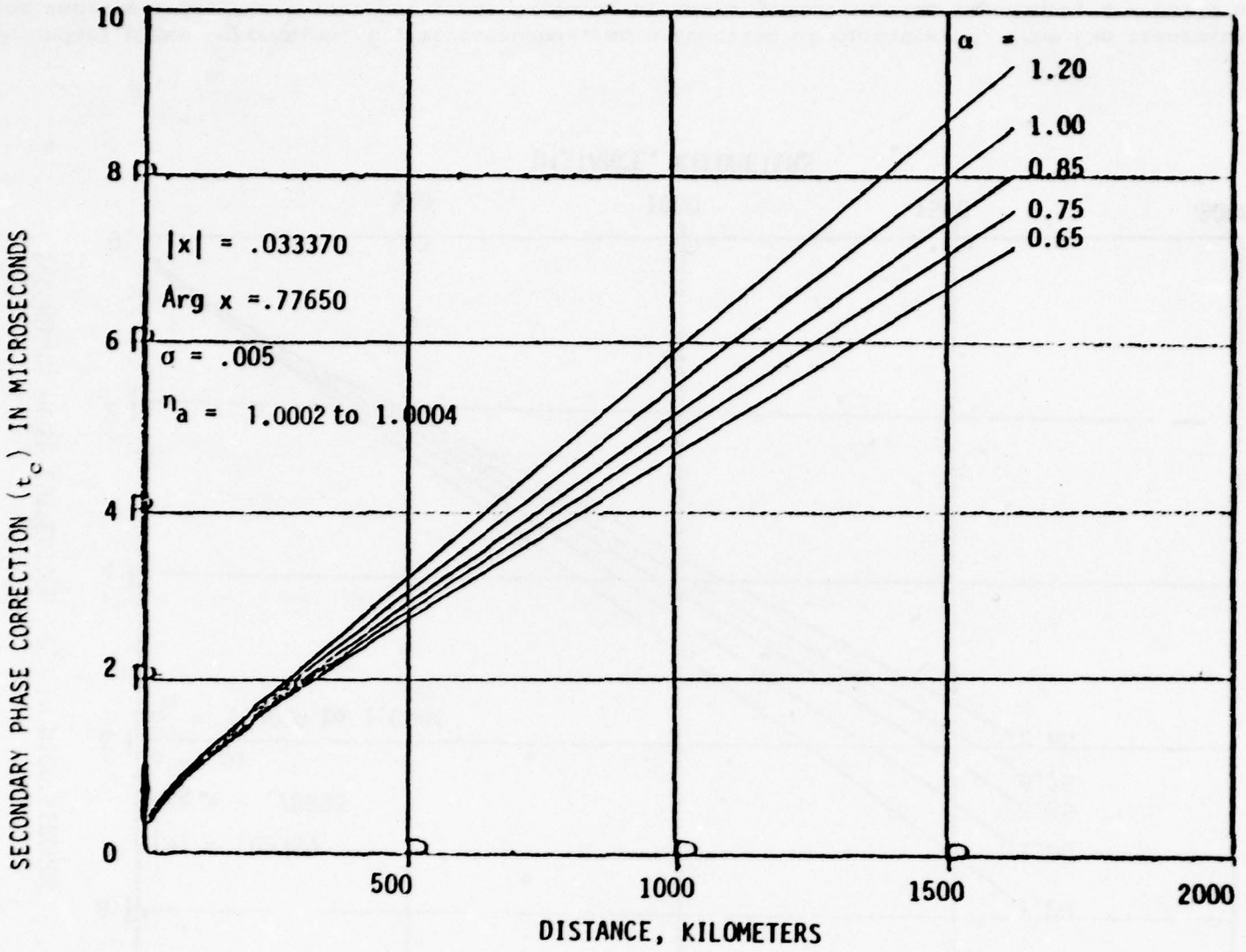

Figure 5 Secondary phase correction, t_c, microseconds, as a function of distance, d, from the transmitter for various atmospheric vertical lapse factors, α and a ground surface impedance, x = .03337 exp (j.77560), and ground conductivity σ = .005 mhos/m (Table 2).

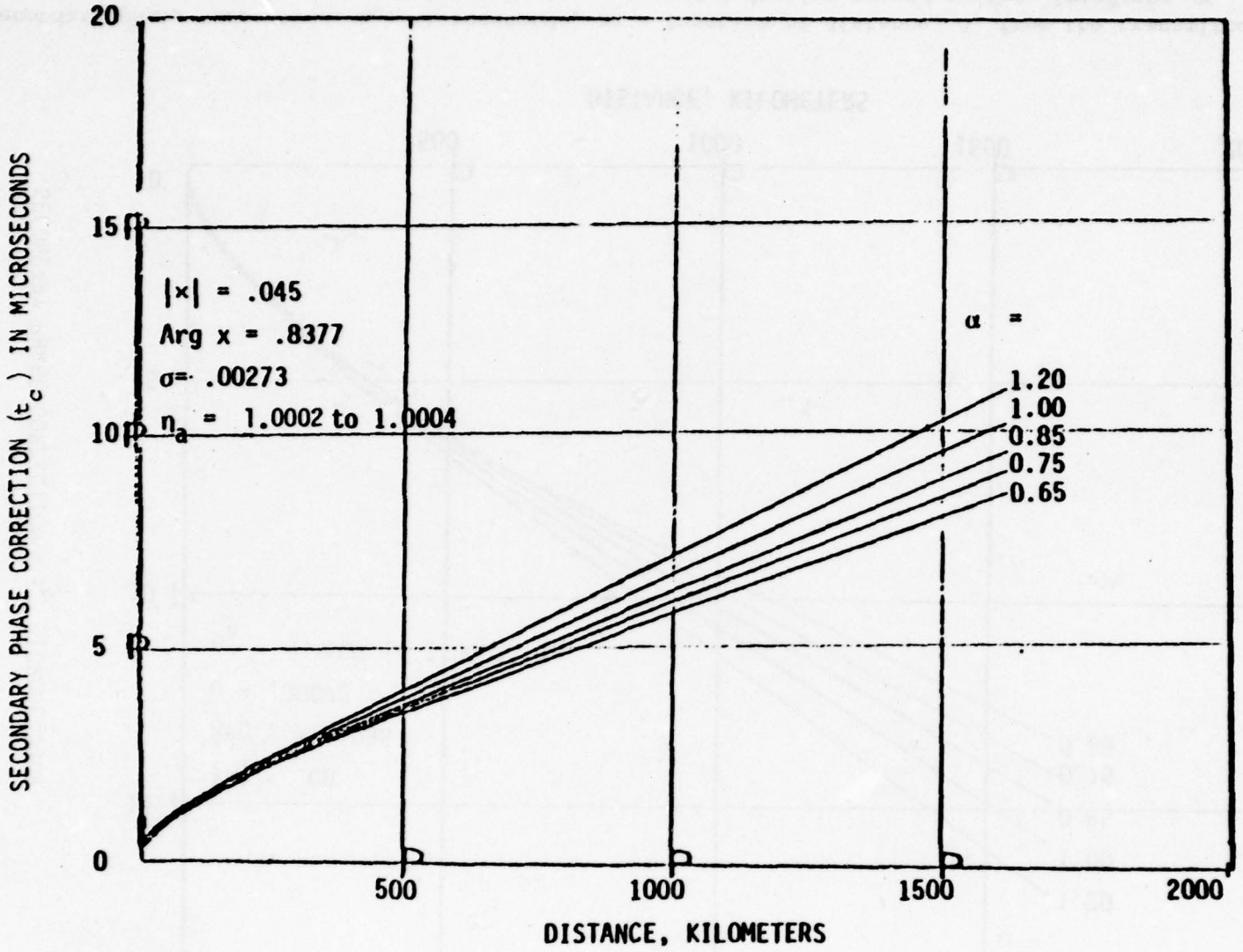

Figure 6 Secondary phase correction, t_c, microseconds, as a function of distance, d, from the transmitter for various atmospheric vertical lapse factors, α, and an inductive ground surface impedance x = .045 exp (j.83770), or a ground conductivity, σ = .00273 mhos/m (Table 2).

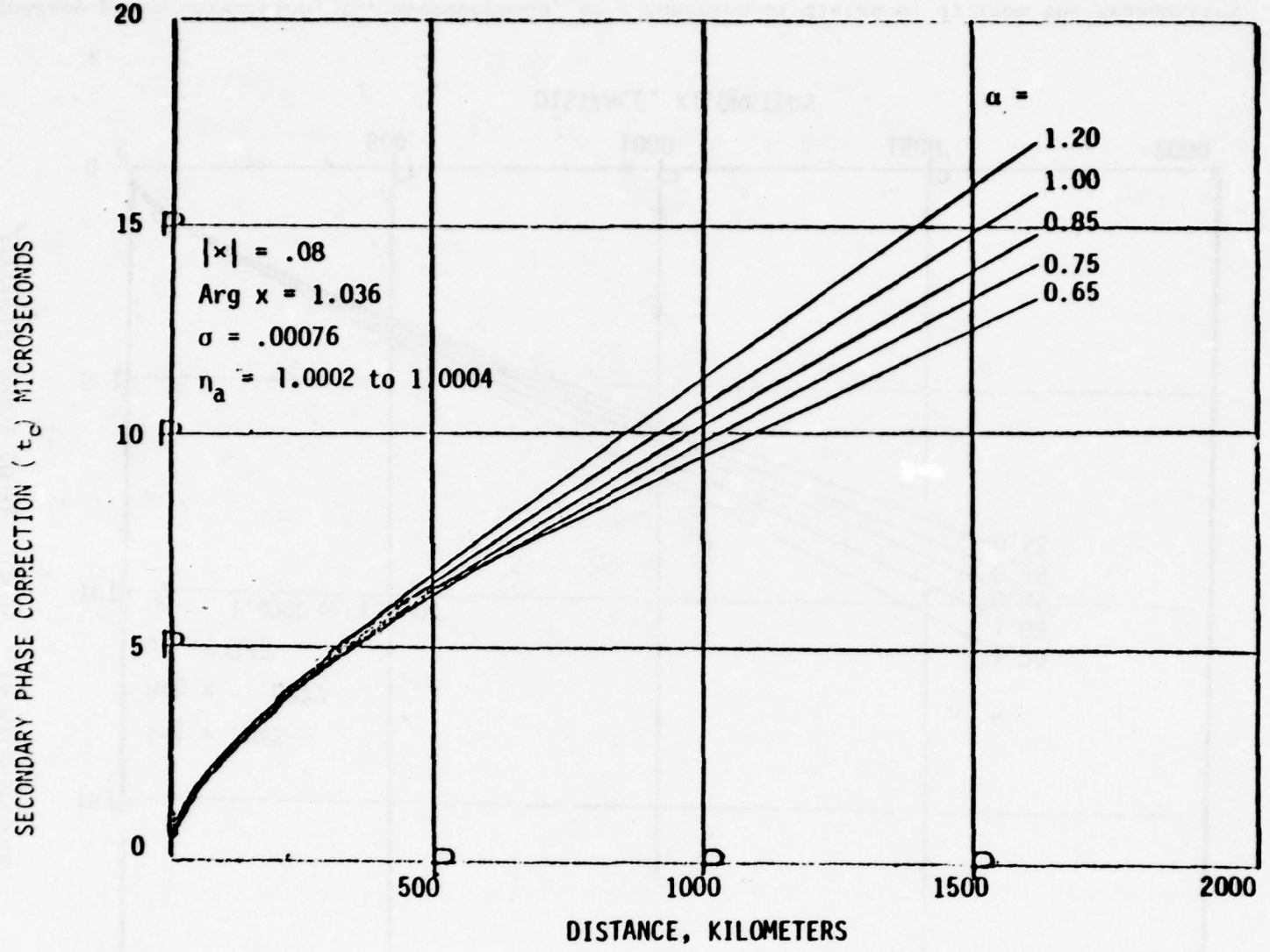

Figure 7 Secondary phase correction, t_c, microseconds, as a function of distance, d, from the transmitter for various atmospheric vertical lapse factors, α, and inductive ground surface impedance, x = .08 exp (j1.036), or a ground conductivity, σ = .0076 mhos/m (Table 2).

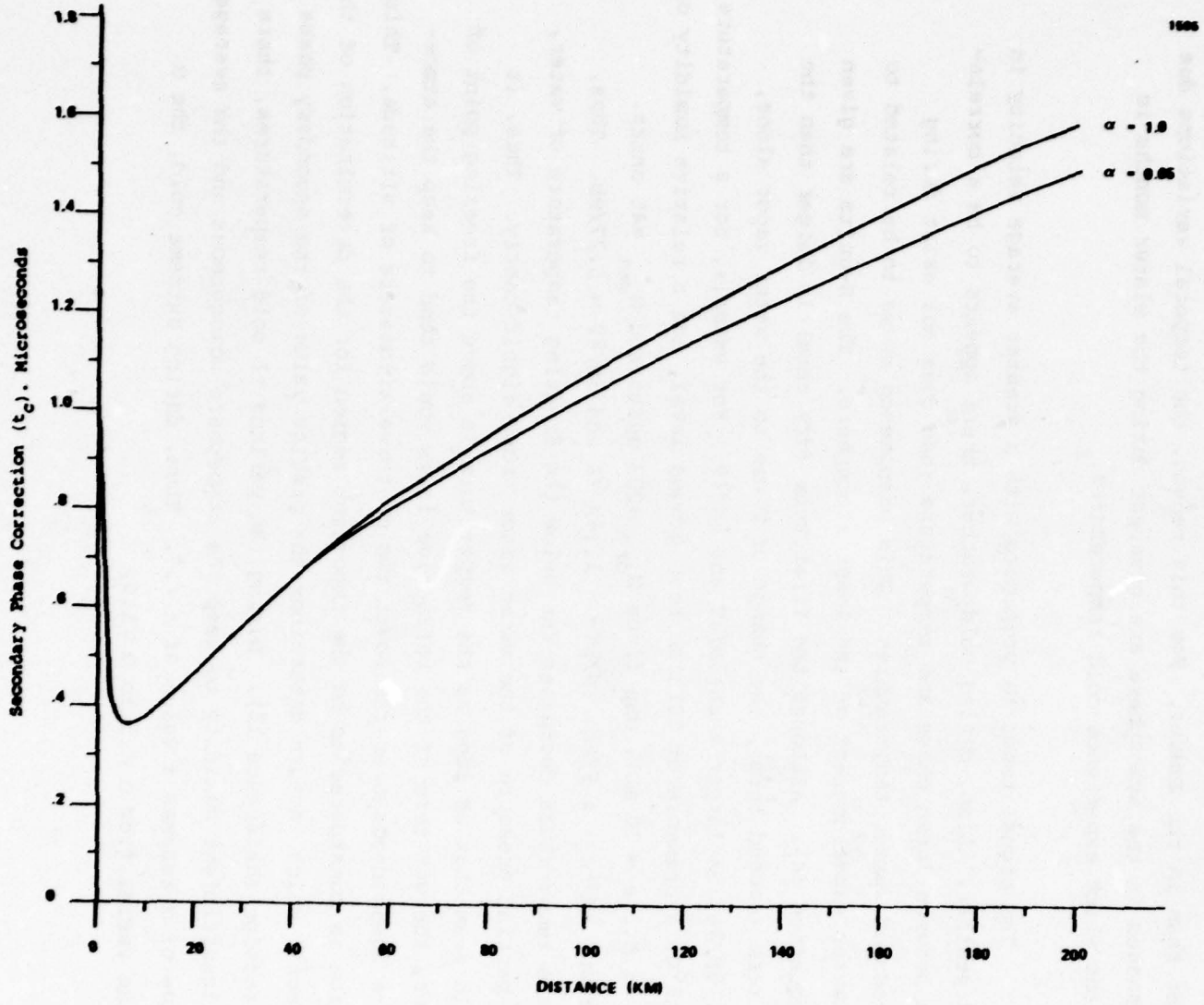

Figure 8 t_C vs Distance for Vertical Lapse Factor (α) of 1.0 and 0.65, for Ground Impedance x = .033 exp (J.77620)

reference (8), can be explained by an α value of 1 $\pm$.02 during the summer months and .70 $\pm$.15 during the winter months. Although the secondary phase correction is least when the temperature is lowest (winter) and corresponding α is lowest, the variation in α is much greater in the winter than in the summer. For this reason, the temporal variations due to changes in the atmosphere are greatest during the winter months in regions which experience cold temperatures.

The signal tends to propagate with a greater average velocity in cold weather. Also, during cold weather, there appears to be a correlation between loran phase and temperature that does not exist during periods of warmer temperatures. This phenomenon seems to be related to the water vapor content of the lower atmosphere. The N-units are given by equation (4). Although the first term (dry term) is larger than the wet term (second term), the change of N due to the water vapor alone, i.e. $\partial N/\partial e$, is larger than $\partial N/\partial T$ and $\partial N/\partial P$. For example, for a temperature of 15^{o}C, a pressure of 1013 mb near ground level, and a relative humidity of 60% (i.e., e = 10 mb), one finds $N_{dry} \simeq 273$ units and $N_{wet} \simeq 45$ units. However, $\partial N/\partial e = 4.5/mb$, $\partial N/\partial T = -1.26/\,^{o}K$ and $\partial N/\partial P = 0.27/mb$. Thus, as the temperature decreases far below the freezing temperature of water, the partial pressure of the water vapor drops significantly. Thus, it would seem that as long as the temperature is above the freezing point of water, the wet term of the refractive index would tend to keep the atmosphere homogeneous over the lower two or three kilometers of altitude. This region is considered to be the important region for the determination of the α factor which in turn determines the precise value of the secondary phase correction (Reference 15). During the periods of cold temperatures, there is insufficient humidity to keep the atmosphere homogeneous and the average value of α assumes a value of a $\sim$.7. Then, during extreme cold, the α value varies from $\alpha \sim .5$ to $\alpha \sim 1.0$.

4.2 Temporal Variation of Propagation Time Due to Ground Impedance Changes.

Techniques for evaluating the ground impedance in the presence of ground horizons at various depths below the surface have been given, reference (6). In general, the impedance, x, is a complex number,

$$x = |x| \exp(j \text{ Arg } x),$$

and can be constructed from values of ground conductivity, σ_1, σ_2, σ_3, ... , dielectric constant, ε_1, ε_2, ε_3, ... , and permeability, μ_1, μ_2, μ_3, ... , for the various ground horizons, provided the electromagnetic boundary conditions between such horizons are applied. Thus, the ground over which the electromagnetic wave propagates is in general nonhomogeneous, not only in the horizontal direction but also in the vertical direction.

The electrical ground conductivity or resistivity at the surface of the ground (i.e., the conductivity of the surface soil horizon) is not always the only important parameter in the determination of the ground surface impedance. The electromagnetic wave penetrates the ground to a considerable depth and in most overland situations one finds that the ground wave is strongly correlated in the space domain with subsurface horizons. Thus, the geologic age and characteristics of the basement rock influences the surface impedance and hence the secondary phase correction.

4.2.1 Graphs Depicting Propagation Time Variation Due to Ground Impedance Changes.

Figures 9, 10, and 11 depict the effect of the ground surface impedance upon the secondary phase correction. The values of effective ground impedance range from

$$x = .001055 \exp(j.7854), \quad \text{(for seawater)}$$

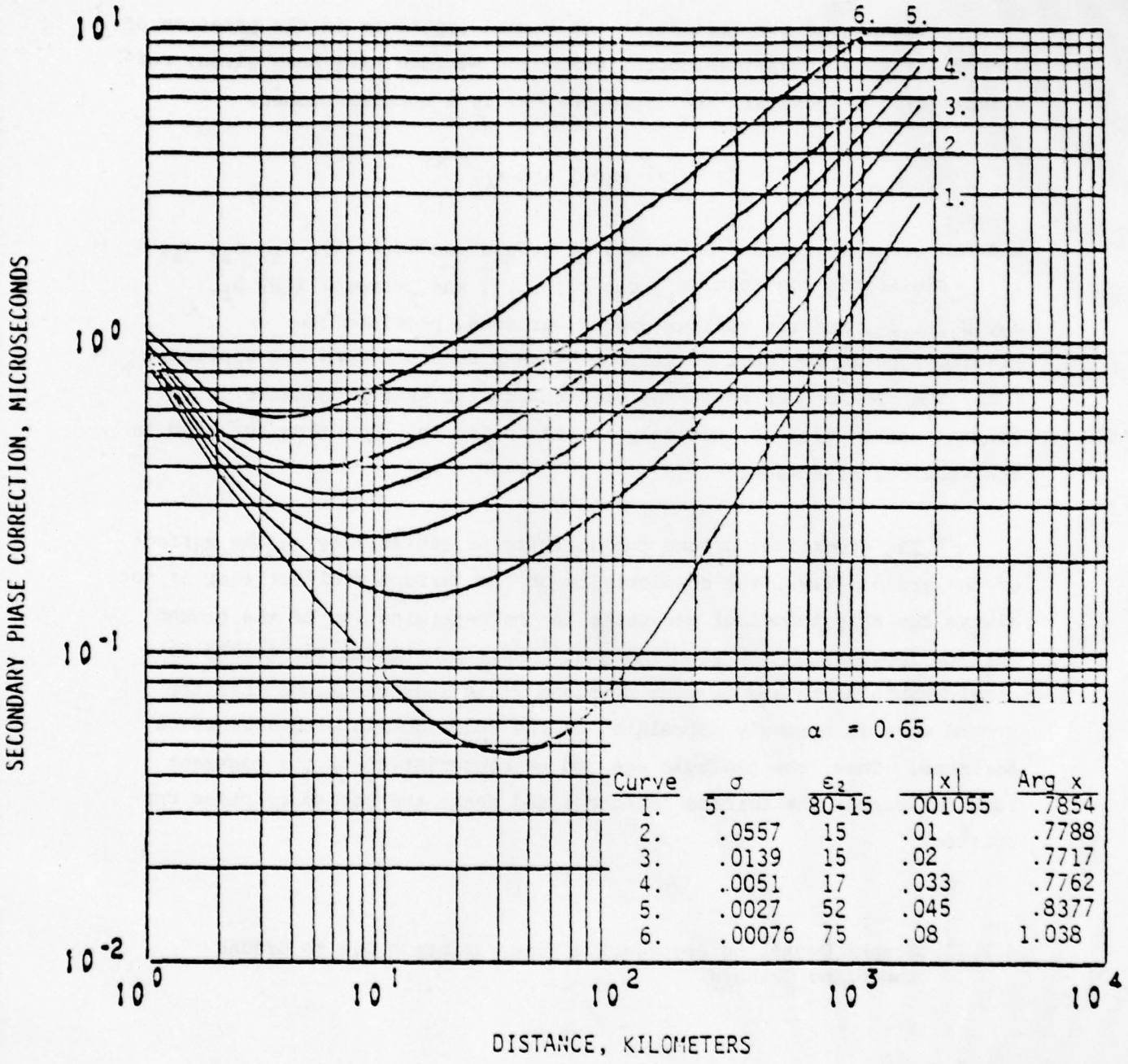

Figure 9 Secondary Phase Correction, t_c, Microseconds as a Function of Distance, d, From the Transmitter for Various Values of Ground Impedance or Conductivity, α = 0.65

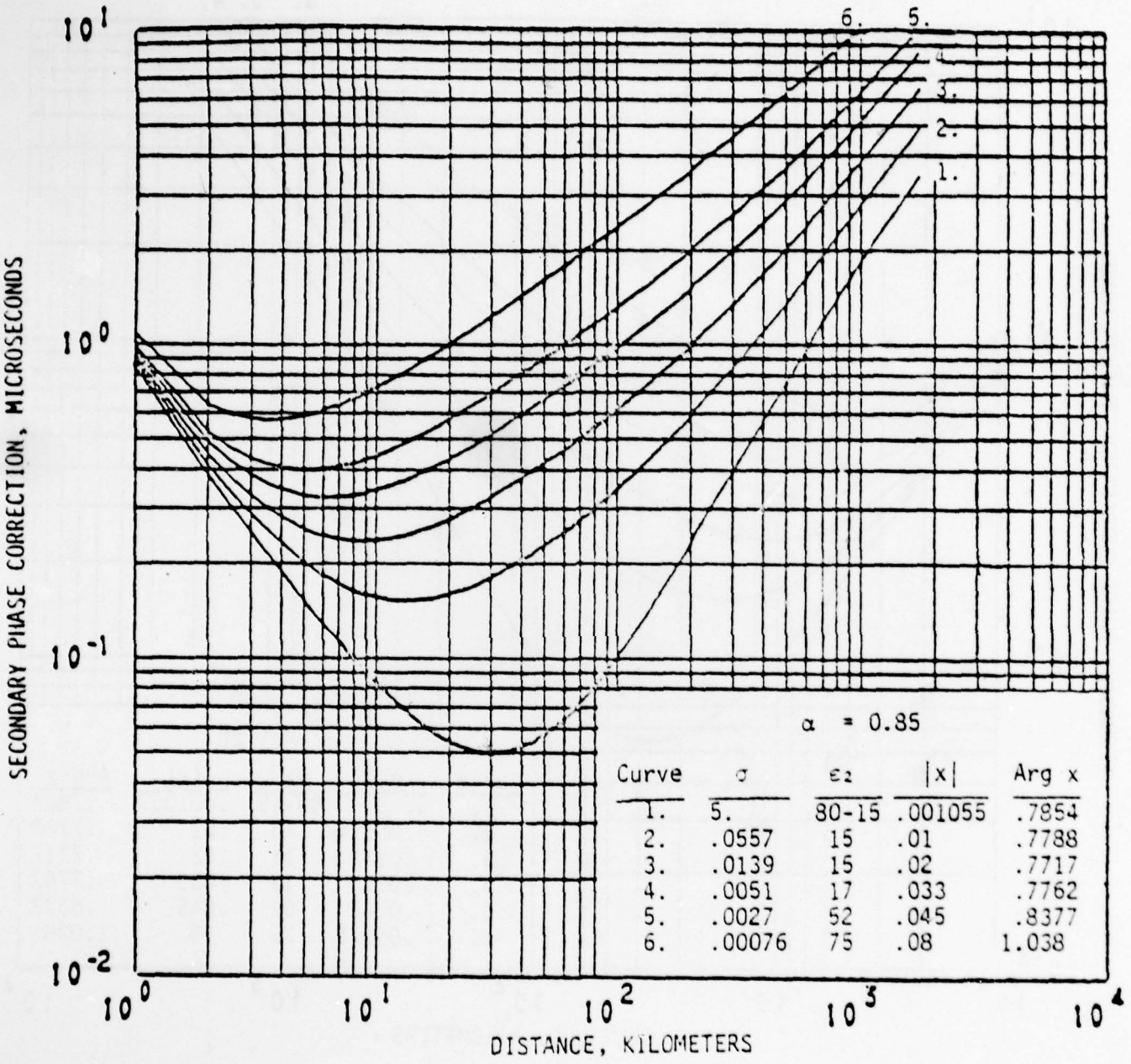

Figure 10 Secondary Phase Correction, t_c, Microseconds as a Function of Distance, d, From the Transmitter for Various Values of Ground Impedance or Conductivity, α = 0.85

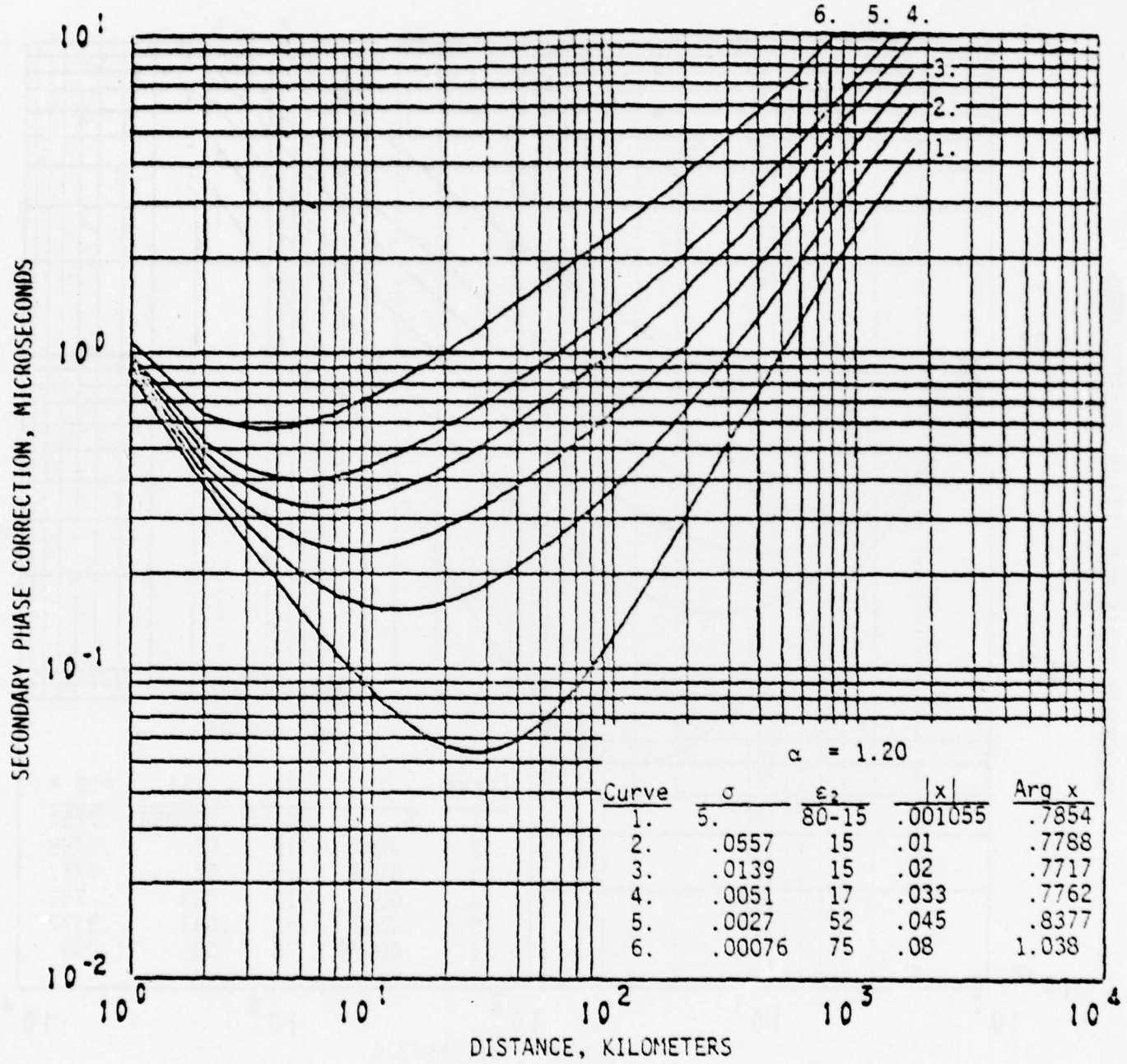

Figure 11 Secondary Phase Correction, t_c, Microseconds as a Function of Distance, d, From the Transmitter for Various Values of Ground Impedance or Conductivity, $\alpha = 1.20$

to an extreme value

$$x = .08 \exp(j1.036), \text{ (for poor earth)}.$$

Vertical lapse factors (α) of 0.65, 0.85 and 1.20 are used respectively for each figure (9, 10, 11). These figures being logarithmic clearly show the effect of varying impedance at short distances (<200 km).

The quantity, $|x|$, is normalized to the impedance of free space (= 377 Ohms), a universal constant of nature, and hence is actually dimensionless. As given in Figures 9, 10 and 11, one can express the effective ground impedance in terms of conductivity, σ, mhos/m and dielectric constant ϵ_2 (relative to ϵ_0 for free space, $\epsilon = \epsilon_2\epsilon_0$). The permeability μ, is of little significance and hence, $\mu = \mu o = 4\pi\ (10^{-7})$ Henry/m. For sea water, $\sigma = 5$ mhos/m. In the extreme case, $|x| = .08$, and the corresponding conductivity $\sigma = .00076$. Effective surface conductivities of $\sigma = .0001$ have not, thus far, been observed in the natural ground of the earth at frequencies near 100 kHz. Conceptually it is difficult to visualize real conditions which would contribute to such low values in effective conductivity. In a real sense, the ground surface effective conductivity, as seen by the electromagnetic wave, is an aggregate of conductivities contributed by the various surface and subsurface horizons extending downward to an order of the skin depth for the wave. The contributing biases from subsurface rocks and soils is sufficient so as to maintain physical boundary conditions at the higher minimum values. Physically, it is highly improbable for contributing sources to permit such low values of effective conductivity. Accordingly, values of $\sigma = .0001$ can be considered nonphysical in so far as the propagation of radio waves which are influenced by the ground is concerned.

The impedance concept embraces all naturally occurring ground electrical properties which have been observed for Loran-C frequencies. Hence, this concept provides a compact generalization of physically realizable electrical properties. Here again and in this concept, effective conductivities like $\sigma = .0001$ are nonphysical and have no meaning for Loran-C. In fact, the curves shown in Figures 9, 10 and 11, when plotted parametric in σ, other parameters being constant, cross over as the

the value $\sigma = .0001$ is approached. Hence the secondary phase correction would decrease instead of increasing as a function of the corresponding impedance. To avoid this nonphysical domain of the complex impedance plane at Loran-C frequencies it is necessary to move the phase angle of the impedance, Arg $x - \pi/4$, to the right in the complex impedance plane. This results, in effect, in a dielectric constant change as shown in Figures 9, 10 and 11. The curves on these figures represent physically realizable values of ground impedance at 100 kHz based upon Loran-C observations in the continental United States, Europe, the Mediterrean and S.E. Asia. These values of impedance can be regarded as effective values over nonhomogeneous and irregular ground. Thus, in lieu of the use of the propagation simulation for nonhomogeneous and irregular ground, Reference (13), practical estimates of Loran-C secondary phase corrections can be obtained from Figures 9, 10 and 11 and experimental data or experience with the Loran-C system. The experimenter and navigator in the field can gain through experience the ability to estimate the ground impedance for any particular propagation path. Also, the physical realizability of a Loran-C observation can be ascertained immediately, especially when gross errors exist in the data. More subtle errors can also be detected with experience. Thus, Figures 9, 10 and 11 present a frame work of theory within which all observations are subject to explanation. However, severely anomalous situations will require the integral equation/full wave for homogeneous and irregular ground, Reference (13).

4.2.2 Example of Temporal Change Due to Change in Ground Impedance

Consider first the nature of the ground in any particular locality as it changes with depth below the surface of the topmost layer of soil. A geoelectric section of the ground between the surface and some depth below (on the order of skin depth) the surface of the topmost soil horizon should be considered in a ground surface impedance estimate. Thus, the waves entering the ground are exponentially attenuated with depth, or distance through the material that comprises the ground, depending upon the conductivity, σ, or the resistivity, ρ. Although the ground is layered geologically, such layering does not necessarily represent an electrical boundary like much clearer air-ground boundary at

the surface of the ground. But the ground does vary in electrical resistivity, ρ_i, dielectric constant, ϵ_i, and permeability, μ_i, i = 1, 2, 3 ... , with depth below the surface. Thus, the ground is anisotropic in the sense that the average resistivity, ρ_i, is different in a direction parallel to the surface as compared to the vertical direction below the surface. The basic quantity that can be used in the ground wave theory of propagation in the atmosphere above the surface of the ground is the ground impedance, x. This quantity represents a value of impedance reflected to the ground-air surface by all of the subsurface material of importance. With the aid of this impedance an electrical boundary condition for the ground wave can be established at the physically obvious air-ground interface. The problem is how to model the region below this interface. Experience has shown, reference (6) that a three layer model is usually the best that can be accomplished in most land areas of the world. There is no theoretical limit concerning the number of layers or geoelectric horizons that can be used. The limit is the availability of geophysical data. Thus, in the three layer model one can use the top soil, the subsoil or hardpan (with water table) and the geologic structure.

This simplified model can be used to illustrate the effect of rainfall upon a desert propagation path between Searchlight, Nevada and Ft. Cronkhite, California. An examination of the geophysical data, reference (6), indicates that under normal dry conditions that are found in the desert, the topmost soil horizon may exhibit great resistivity while the second horizon is saturated by the water table. The bedrock is often very high in resistivity. The topmost horizon comprising only a very few meters is subject to sudden changes during heavy rainfall. If this weather is extensive or covers a large portion of a propagation path, changes due to ground impedance may be observable.

Typical conditions along the propagation path over the desert in terms of a three horizon model is a 6 meter top horizon, $\sigma_1 = .0005$, below which is a water table horizon, $\sigma_2 = .01$, with a thickness of 10 meters. The bedrock can be assigned a conductivity, $\sigma_3 = .0005$. The corresponding value of surface impedance for desert values from Table 4 is:

$$x = 0.0325 \exp\left[j.7646\right]. \quad \text{(case A)}$$

TABLE 4

GROUND IMPEDANCE FOR THREE HORIZON MODEL

USING TYPICAL VALUES FOR DESERT REGION

CASE	σ_1	σ_2	σ_3	W_1	W_2	$\|x\|$	Arg x
B	.0005	.01	.01	6	10	.03320	1.0230
A	.0005	.01	.0005	6	10	.03254	.7646
	.0005	.01	.0036	6	10	.03312	.9221
	.002	.005	.00054	2	10	.0418	.4939
	.01	.01	.04	1	2	.0154	.9596
	.067	.067	.067	1.5	10	.00914	.7847
C	.01	.01	.01	1	2	.0236	.7810

σ_1 = Conductivity of top most horizon of soil

σ_2 = Conductivity of second soil horizon

σ_3 = Conductivity of bedrock

W_1 = Thickness, meters of top most horizon of soil

W_2 = Thickness, meters of second soil horizon

$W_3 = \infty$

An increase in the conductivity of the geologic structure to a value, σ = .01 would reflect a ground surface impedance of $x = .0332 \exp\left[j1.023\right]$ (case B). This is a highly inductive ground because the phase angle is considerably greater than $\pi/4 = .7854$. Suppose heavy rainfall causes the topmost horizon to reach a conductivity $\sigma = .01$. Then, from Table 4 calculated values we find:

$$x = .0236\left[\exp j.7810\right] \quad \text{(case C)}$$

Referencing Figure 12, using Arg $x - \pi/4 = -.0044$ radians (case C), $t_c \sim 4.20$ μs (microseconds) for a 1000 km propagation path. Also, $x = .033$ using Arg $x - \pi/4 = .238$ (case B) gives, $t_c = 5.00$ μs or a change of about 0.80 μs. This is a very great change and it is clearly physically possible but perhaps not probable under normal weather conditions.

The method for calculating x in the three or more horizon model is given in reference (6). It is interesting to note that a path in the complex impedance plane which follows $|x| = .001$ and Arg $x - \pi/4 = 0$ (or slightly negative) up to a value of $|x| = .03$ and then moves to positive values Arg $x - \pi/4$ up to a value of $1.036 - .7854 = 0.251$ radians at $|x| = .08$ can be used to explain most Loran-C phenomenon in terms of secondary phase correction. This, of course, is a pragmatic simplification and leads to the set of curves given in Figures 9, 10 and 11. Thus, Figures 9, 10 and 11 reduce a comparatively complex technology to a simplified form which can be used to analyze and better to understand Loran-C coordinate observations or Loran-C propagation time observations (TOA's).

Table 5 gives values of t_c', where

$$t_c' = \partial t_c / \partial d, \text{ ns/km}$$

parametric in the impedance magnitude, $|x|$, and the vertical lapse factor α. The corresponding values of ground effective conductivity, σ, are also given. These values are derived from numerical values presented in Figures 9, 10 and 11, between 1000 and 1800 km.

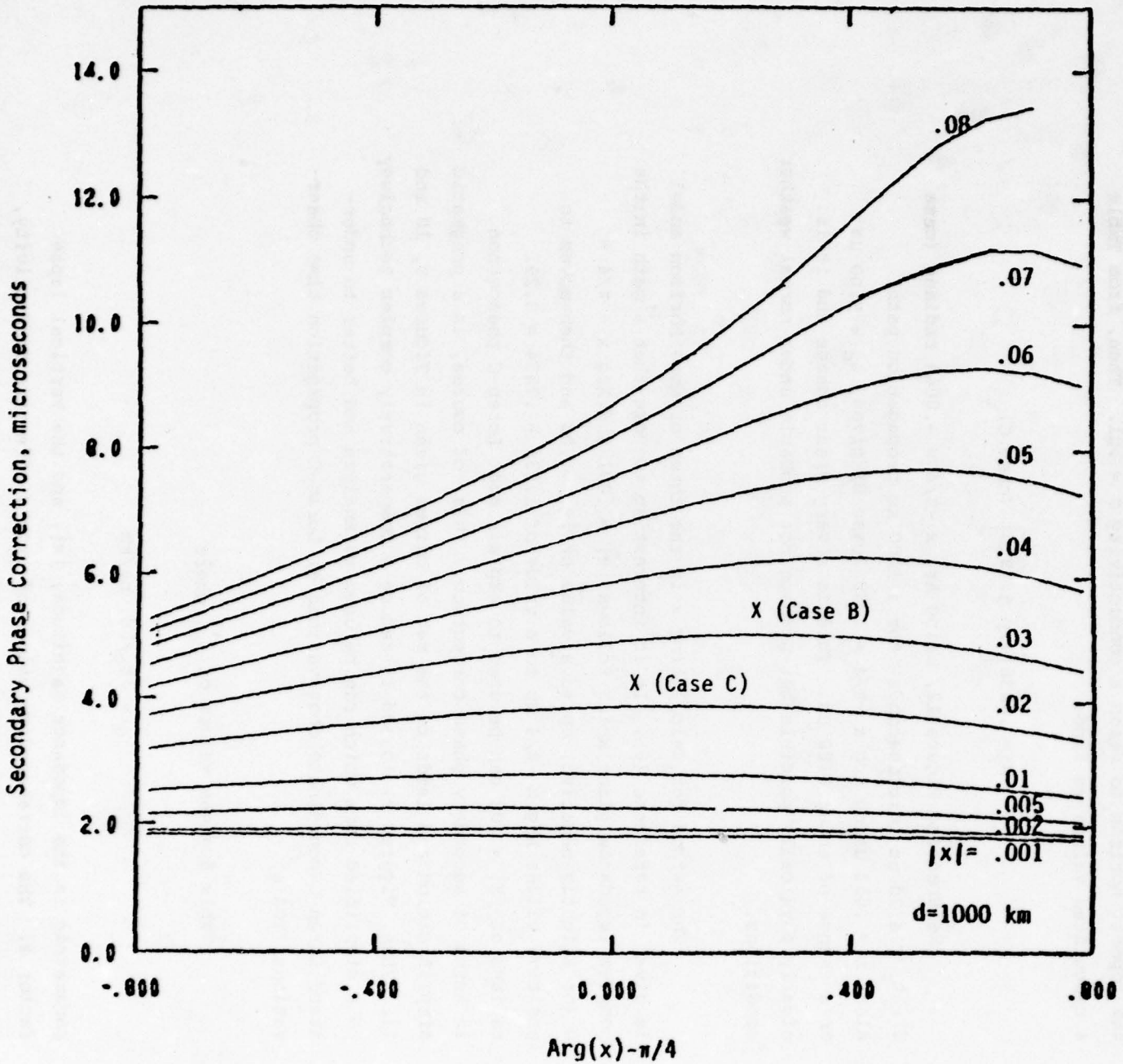

Figure 12 Secondary Phase Correction, in, Microseconds, for a Ground Wave Propagated to a Distance, d = 1000 km, as a Function of the Complex Ground Impedance, $x^{(a)}$ = 0.001 to 0.08 and $x^{(p)}$ - π/4 Values Between -0.8 & +0.8 Radians

TABLE 5

RATE OF CHANGE IN SECONDARY PHASE CORRECTION, t_c', NANOSECONDS PER KILOMETER, FOR VARIOUS IMPEDANCE MAGNITUDES, $|x|$ AND VERTICAL LAPSE FACTORS, α.

$\|x\|$	α	t_c', ns/km	α	$\|x\|$	σ	t_c', ns/km
033	.5	3.497	5	.001055	.85	2.233
	.55	3.675	.0557	.01		2.940
	.60	3.844	.0139	.02		3.701
	.65	4.011	.0051	.033		4.608
	.70	4.168	.0027	.045		5.420
	.75	4.320	.00076	.08		6.048
	.80	4.466				
	.85	4.608				
	.90	4.746				
	.95	4.880				
	1.00	5.011				

It is of interest to note that a $\pm$ 18% change about α = .85, between α = .70 and α = 1.00 produces a change in secondary phase correction derivative, $\Delta t_c'$ = .843 ns/km. Also, a 36% change in the impedance $|x|$, between $|x|$ = .033 and .045 produces a change in secondary phase correction derivative, $\Delta t_c'$ = .812 ns/km. The corresponding change in the ground effective conductivity parameter, σ, is 47%. It thus appears that the impedance magnitude changes and the α-factor changes produce the same order of magnitude change in secondary phase correction whilst the conductivity must change about 11% more to produce an equivalent change. Thus, σ is less sensitive than $|x|$ and α in producing phase variations. In this we have assumed the variations are about average values α = .85 and/or $|x|$ = .033.

Figures 9, 10 and 11 contain information to that available on $CRPL_1$ small desk top calculator computer programs using polynomial representation. These computer programs can be used to derive effective impedances for mixed paths using the Pressy, Ashwell Fowler method, (Reference 24). Table 6 gives sample calculations for three segment propagation paths using these computer techniques.

TABLE 6

SAMPLE CALCULATIONS FOR MIXED PATHS

Segment No. 1 |x|,Δd(km)	Segment No. 2 |x|,Δd(km)	Segment No. 3 |x|,Δd(km)	t_c Micro Seconds	|x| Effective
.001,100	.045,100	.033,100	1.525	.0233
.033,100	.045,100	.001,100	1.525	.0233
.001,300	.02,300	.08,300	5.126	.0368
.08,300	.02,300	.001,300	5.126	.0368

Thus, combining three segments 100km in length each yields a secondary phase correction of 1.525 microseconds at 300 km or an effective impedance of .0233 if the segment impedances are .001, .045 and .033, respectively. Reversing the order, of course, gives the same result. Using 300 km segments and values of each segment of .001, .02 and .08 respectively gives a secondary phase correction of 5.126 microseconds and an effective impedance value of .0368. Thus, all of the mixed path wisdom including the net path impedance values are contained in Figures 9, 10 and 11 when programmed into a small calculator.

5. APPLICATIONS OF RESULTS

5.1 Software Program for User

One of the goals of this development is a portable inexpensive machine which will be able to calculate a secondary time delay as frequently as the situation warrants with only a few numbers required to be supplied by the user.

The general calculation for the secondary phase correction of the ground wave portion of a LF electromagnetic signal is an intricate calculation which requires machine computation. Many experimentally determined numerical values must be available that require storage allocation which is presently only available on large machines. By using appropriate average values for some of the required data the calculation can be performed on a smaller machine and hopefully result in correction for the secondary time delay of propagation which will be beneficial as a first approximation to the Loran-C user. A FORTRAN-IV program has been developed which performs the required calculation for ranges > 10Km with a 50 nanosecond accuracy and uses only a moderate amount of storage space. A flow diagram of this program is given in Figure 13. The Coast Guard has expressed an interest in having such a program for use on the Hewlett-Packard HP9825 desk-top calculator. A listing of the Software for Functions FAMP and TC and Subroutine GROUNE is given in Appendix A. This listing is in FORTRAN-IV language and requires translation to Hewlett-Packard language. In addition, an Executive Main Calling program is required.

To make this calculation tractable, parameters in the general model, which introduces effects due to terrain roughness, soil stratification, soil consistency, geological underlayment and surface elevation have been eliminated.

The parameters of importance which have been retained are:

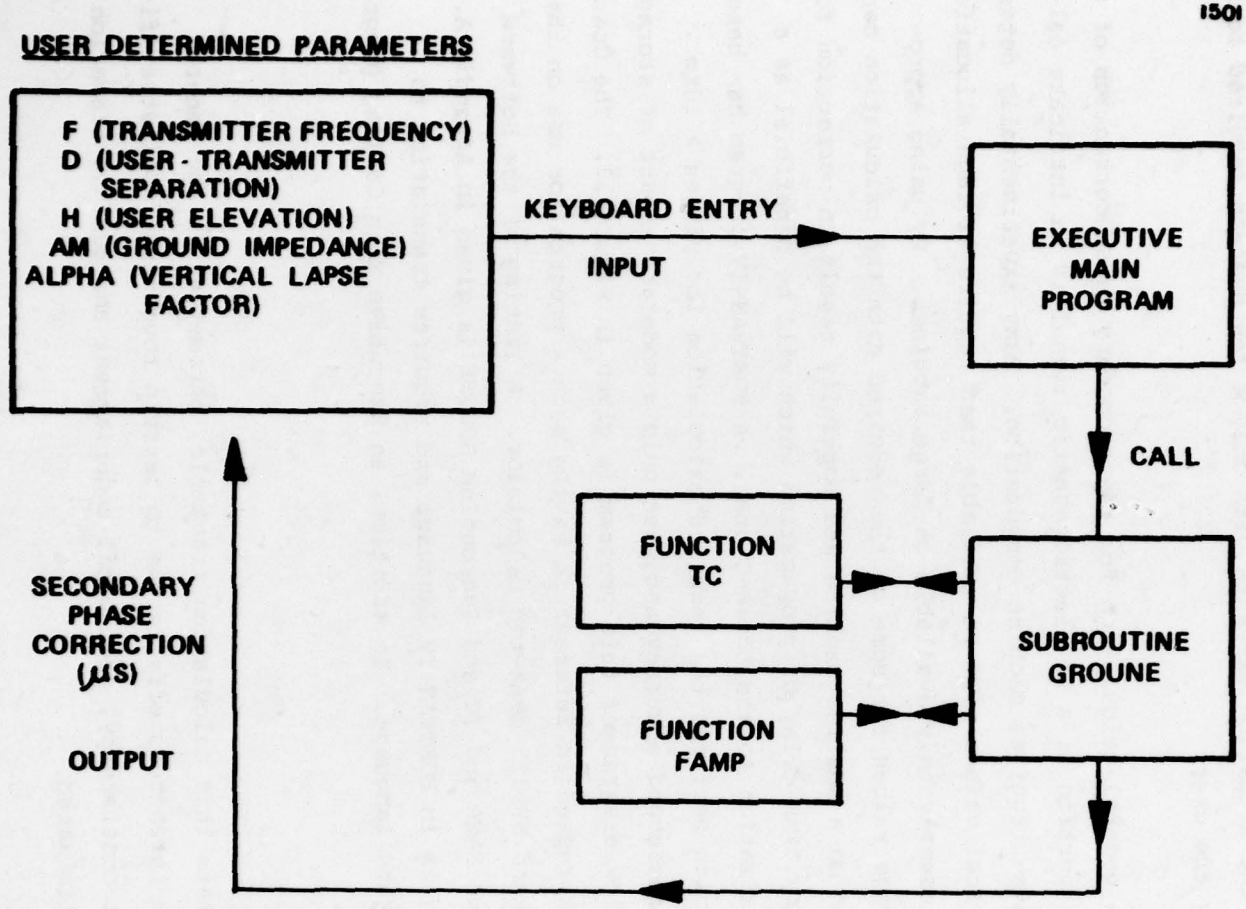

Figure 13 User Interactive, FORTRAN-IV Flow Chart for Calculation of Secondary Phase Correction of Loran-C

A) Frequency of relevant Loran-C transmitter

B) Distance of separation between transmitter and user

C) User elevation above surface.

D) Index of refraction of air at surface.

E) Impedance of surface.

F) Vertical lapse factor for index of refraction.

The first three parameters are scalar's. Parameter A is known exactly. Parameters B and C can usually be adaquately determined to the first order.

The remaining three parameters are of a more complex structure, being non-uniform spatially and temporally. In the general model parameters D and E, which have a two dimensional spatial dependence, are defined separately at each node of a specified grid, being in part responsible for the large storage requirements. Parameter F, in general, has a three dimensional spatial variation due to possible inversion layers in the atmosphere. Numerical data describing this parameter, since it is transient, is usually not available.

Of these six remaining parameters all except D and E are therefore the same as in the general model, while D and E are introduced as single scalar quantities.

The index of refraction of the air at the surface is known to be a function of temperature, atmospheric pressure and the partial pressure due to the water vapor content of the atmosphere. The empirically observed numerical value lies between 1.0002 and 1.0004 and in the abbreviated program, the parameter has been built in, (therefore need not be entered by the user) with the constant value of 1.000338. This is the value usually used for the average propagation time calculation of the primary wave.

The ground impedance values corresponding to the amplitude, $|x|$, and phase, arg x, given in Table 1, comprise a subtle generalization that permits considerable simplification of practical Loran-C predictions and demonstrates a specialized use of the general impedance concept to Loran-C

that has been found to be useful throughout the world. The application of the impedance concept is based on observations and the original observations were derived in References 17, 18, 19 and 20.This concept has been successfully used in a variety of Loran-C applications. Since this time, further use of the impedance technique to analyze data using small programmable computers have been given in References 21, 22 and 23. The method is readily adapted (as demonstrated in the above references) to small, portable programmable calculating predictions.

The vertical lapse factor is known to vary in general between 0.60 and 1.20 due to weather conditions. For the abbreviated model, values between 0.70 and 1.0 are acceptable inputs.

In summary: the present abbreviated program will require that the user enter five numbers (A, B, D, E, F) from a keyboard entry device, and it will output a single number, the secondary phase correction in microseconds, which can be applied as a first approximation to correct for position location on the usual Loran-C hyperbolic grid system.

5.2 Assessment of Impact on Loran-C Chain Control

Monitoring and fine-timing adjustments of Loran-C Signals are performed by a System Area Monitor (SAM). The System Area Monitor has receiving equipment, usually located remotely, to continuously monitor the relative timing between master and secondary station transmissions. The SAM's normal function is to issue timing adjustments to the secondary station (Local Phase Adjustment, or LPA) to compensate for any frequency offset of the secondary station oscillator with respect to the master station oscillator, and includes propagation variations. These adjustments maintain the phase (cycle) time-difference at the assigned value (Controlling Standard Time Difference, CSTD).

The total adjustment thus contains both the oscillator drift and the temporal propagation variations along the path between the secondary

stations and the SAM. This approach enhances the accuracy of a user navigating with Loran-C in the vicinity of SAM. However, because the Loran-C chains and SAM's are necessarily land-based; the typical user is quite far away, i.e. on the ocean or in harbors or estuaries. Thus the part of the timing adjustment which is attributable to temporal propagation variation over the transmitter-SAM path is not applicable over the transmitter to user path and its inclusion deteriorates the navigation accuracy of the user.

Therefore, if the temporal propagation variations at the SAM can be separated from the total timing variation, it would be possible to make adjustments which would compensate for oscillator drift alone.

6. VALIDATION OF RESULTS

In order to validate the results presented in this report, it is recommended that data be collected at a site (possibly a System Area Monitor) where knowledge of the electrical characteristics of the propagation path is fairly well understood and in a geographic location where extreme weather conditions are experienced (i.e., Northeast United States).

The secondary phase correction can be calculated when the ground impedance, x, (or conductivity and dielectric constant) of the propagation path and the vertical lapse factor of the refractive index, α, are known. If the electrical characteristics of the propagation path are known, then the vertical lapse factor becomes the most important parameter to be derived.

To determine α, knowledge of the temperature, atmospheric pressure and partial pressure of water vapor are needed both on the surface and at an altitude of ~ 2 km. Optimally, both the surface and altitude values should be measured. If only the surface values are available, it will be necessary to develop some typical vertical profiles for various climactic conditions. Also, the immediate history of the surface values of T and e may be used to determine appropriate lapse rates.

Using these measured (or derived) values of α along with continuous recordings of Loran measurements the experimenter can relate α with measured phase changes and validate the results presented in this report. Ideally all measurements should be made throughout the 24 hours of the day and throughout the four seasons of the year.

Figure 14 illustrates in an analytical block diagram a receiver/processor system to compensate for secondary phase error due to meteorological effects such as temperature and pressure.

Although the block diagram shows propagation corrections being sent back to the SAM for cesium corrections, this system could very well be used to improve the fix of a moving platform.

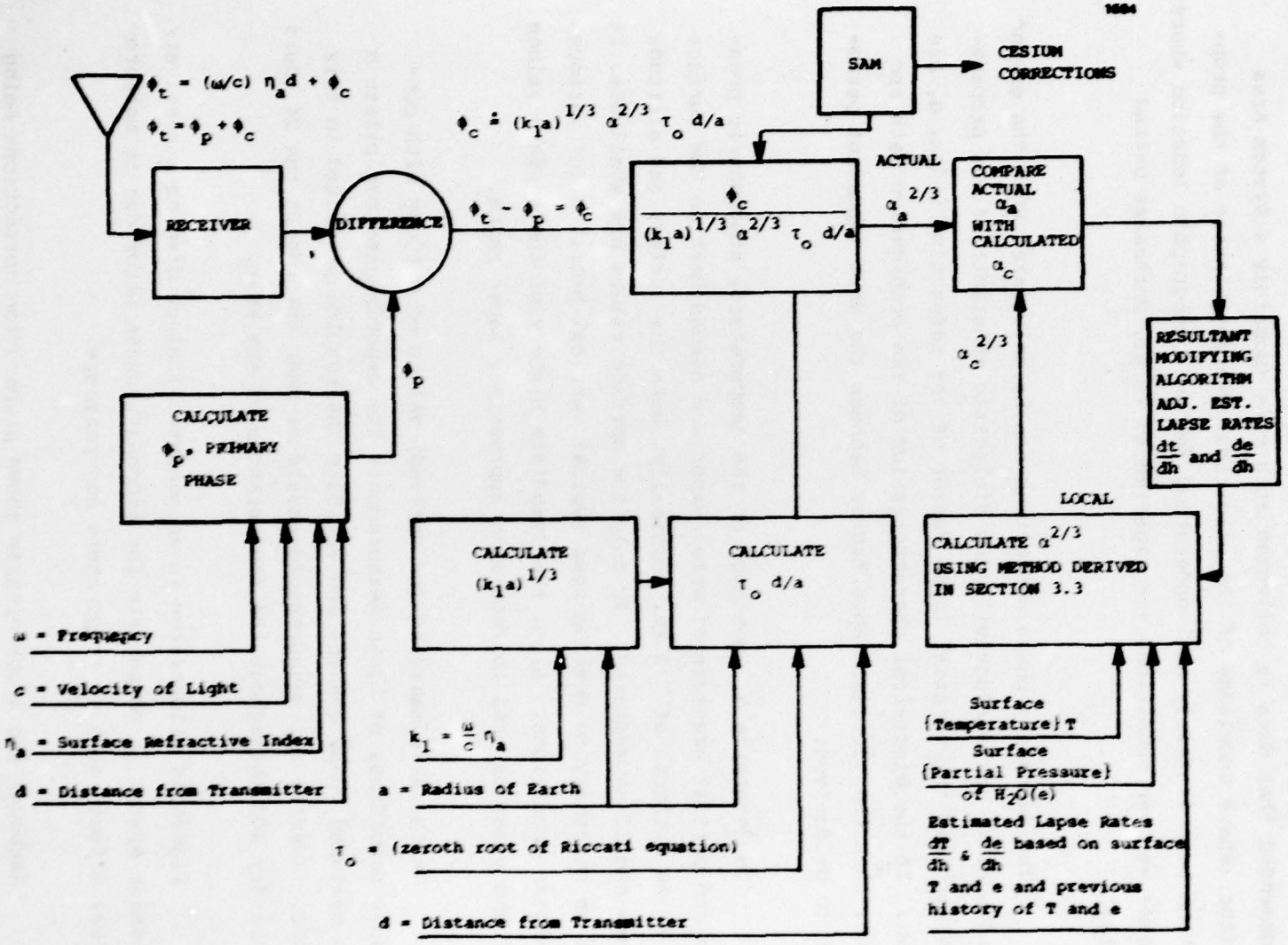

Figure 14 Validation Analytical Block Diagram

To understand how this system operates, consider the familiar expression for the phase of a low frequency radio signal:

$$\phi = \frac{\omega}{c} \eta_a d + \phi_c \qquad \text{(Radians)}$$

This expression has two components, ϕ_p (primary phase) and ϕ_c (secondary phase). ϕ_p is calculated from:

$$\phi_p = \frac{\omega}{c} \eta_a d \qquad \text{(Radians)}$$

and ϕ_c is calculated from:

$$\phi_c = (k_1 a)^{1/3} \alpha^{2/3} \tau_o \frac{d}{a} \qquad \text{(Radians)}$$

where α is developed from a meteorological relationship given by Bremmer, H., 1949 for 0°c and modified by Dr. S. N. Samaddar for general use:

$$\alpha = 1 + a \times 10^{-6} \frac{dN}{dh}$$

$$\frac{dN}{dh} = -\left[\frac{776 \times 1.268}{T} + \frac{77.6}{T^2}\left\{P + \frac{9620e}{T}\right\}\frac{dT}{dh} + \frac{77.6}{T}\left(1 - \frac{4810}{T}\right)\frac{de}{dh}\right]$$

where e = partial pressure of water vapor (millibars)

T = Temperature (° Kelvin)

P = Total pressure in millibars

h = Height in meters

The primary phase (ϕ_p) can be calculated in a straightforward way at a fixed SAM site, assuming distance (d) is known accurately. For a moving platform, distance becomes a dependent variable to be calculated, and updated, via the closed loops around the ϕ_p and ϕ_c processes.

It is interesting to note that at a SAM, e and T may not be known over the entire path. However, dt/dh and de/dh are the parameters of importance and they can be determined at the SAM, one point on the path. In a moving vessel, the navigator can acquire e and T not only along some segment of the propagation path, but also as a function of time. Implementation of this system (Figure 14) using these new data may improve his accuracy. The reader is directed to Section 4.1.2 for a more detailed explanation of the function of meteorological effects upon Loran-C accuracy. It appears that predicted accuracies less than 50 feet may be realizable when processors sense ambient meteorlogical conditions to fully reap the benefits of Loran-C.

7. CONCLUSIONS AND RECOMMENDATIONS

7.1 Conclusions

The most important parameter of concern in temporal variations is the atmospheric vertical lapse factor α. This factor can be related to the surface refractive index η_α, which directly affects the primary wave phase correction. Due to its correlation with the α factor, η_a affects the secondary phase correction only indirectly. Most observable temporal changes due to the atmosphere can be taken into account between values of $\alpha = 0.60$ to 1.20.

The changes in secondary phase correction are proportional to $\Delta(\alpha^{2/3})$ and Δd (increments of two thirds power of alpha and distance). The effect of $\Delta\alpha^{2/3}$ increments is more pronounced at greater distances because of the linear increase with distance as a multiplicative factor. However, the variations in α are greater in the winter months than in the summer. Temporal variations in observations along a 1000 km path in the eastern U.S. can be explained by an α value of 1.0 ± 0.2 during the summer months and $.70 \pm .15$ during the winter months.

The secondary phase correction is most sensitive to the electrical constants of the ground impedance, x. Values of the magnitude of the impedance range between $|x| = 0.001055$ for sea water to $|x| = .08$ for typical areas of the continental United States, Europe and parts of Asia. The latter value of impedance is inductive in nature and corresponds to a conductivity, $\sigma = .00076$ mhos/m with an accordingly adjusted value of dielectric constant. Temporal variations can also occur due to a change in the impedance of the ground due to precipitation. Although, as described in the example described in Section 4.2.2, a change of 0.8 μs is theoretically physically possible, it is not considered probable under normal weather conditions.

A flow diagram for a computer program to calculate the secondary phase correction is given in Section 4.3. This program provides an

accuracy of 50 nanoseconds and a listing is available in FORTRAN IV language, (Appendix A).

7.2 Recommendations

It is recommended that α variations be established by using meteorological data for different altitudes at any given location. Loran-C data should be analyzed using this value of α.

It is recommended that the aforementioned program be translated to Hewlett-Packard language for use on the HP9825 desk calculators normally used by the Coast Guard. This will aid both in evaluating the effects of temporal induced errors on Loran-C accuracy, and in implementing chain control techniques.

As mentioned in the objective, area monitors are used to control the Loran-C chains but the propagation temporal changes removed at the geographic location of the monitor are not appropriate for some other location. The use of the above mentioned computer program might be useful for the SAM for calculating (out of the timing corrections) the secondary phase correction for his unique location. This program might also be useful for the user for calculating the secondary phase correction unique to his location.

Lastly, it is recommended that a study be made to investigate the possible use in the future of the NAVSTAR Global Positioning System (GPS) for Loran-C chain control (in lieu of applying propagation corrections to the present control techniques). GPS provides extremely accurate three-dimensional position data, velocity information and system time to a user. The purpose of the recommended study is to determine whether this type of information will improve upon the current Loran-C chain control provided by the SAM. The present system corrects for errors only in the geographical area of the System Area Monitor while all other areas become degraded. Using GPS, all of the chain area would be treated equally and improvement in overall accuracy might be realizable.

REFERENCE

1 "National Plan for Navigation", U.S. Dept. of Transportation, November 1977

2. Eaton, R.M. Mortiner, A.R., Gray, D.H. "Accurate Chart Latticing for Loran-C", Canadian Hydrographic Service

3. Illgen, J.D., Nelson, L.W., "Loran-C Signal Analysis: Time Varying Components of Loran-C Equipment and Propagation Induced Errors", Private Communication, 1978

4. Johler, J.R., Kellar, W.J., Walters, L.C., "Phase of the Low Radio frequency Ground Wave", NBS Circular 573, 1956

5. Johler, J.R., R.H. Doherty, "Temporal Effects of Natural Origin in Loran-C Ground Wave Propagation", CRPL; Report 79-1, 1 May 1979

6. Johler, J.R. "Geophysical and Geological Data Base Evaluation for Loran-C Ground Wave Propagation Medium", CRPL; Report 78-9, 1978

7. Samadder, S.N. "The Theory of Loran-C Wave Propagation -- a Review" (U.S. Coast Guard, G-DOE-4, TP54, Washington, D.C. 20590; presented at 1978 Helsinki Conference of URSI; to be published).

8. Doherty, R.H. and J.R. Johler "Meteorological Influences on Loran-C Ground Wave Propagation"; Jour. of Atm. and Terr. Phys. 37, 117 to 1124, 1979

9. Doherty, R.H. and J.R. Johler "Analysis of Ground Wave Temporal Variations in the Loran-C Radio Navigation System," OT Technical Memorandum 76-222, (U.S. Dept. of Commerce, OT/ITS, 325 Broadway, Boulder, Co. 80303), 1976

10. Dean, W.N. "Diurnal Variations in Loran-C Groundwave Propagation" (Magnavox Government and Industrial Electronics Company, Fort Wayne, Indiana), 1978

11. Bean, B.R. and G.J. Dutton, Radio Meteorology, NBS Monograph 92, (Suptd. of Doc., U.S. Gov. Print. Off., Washington, D.C. 20402), 1966

12. Doherty, R.H. "Spatial and Temporal Electrical Propagation Measurement", AGARD Conference Proceedings No. 144, 1974.

13. Johler, J.R. "Loran-C Ground Wave Secondary Phase Corrections Over Nonhomogeneous and Irregular Ground Using Transient Signal Propagation Techniques", CRPLi Report 78-12, (U.S. Coast Guard Contract DOT-CG-8429323A, U.S. Coast Guard Headquarters, Washington, D.C. 20590; Prepared by: Colorado Research and Prediction Laboratory Inc.) 1979

14. Nelson, L. and E. Feniger (1978), "Loran-C Signal Analysis: Stability Experiment Summary Status Report", GE 78 TMP-56 (General Electric-TEMPO, Center for Advanced Studies, Santa Barbara, California).

15. Samaddar, S.N., "Weather Effect on Loran-C Propagation," U.S. Coast Guard (to be published), 1979.

16. Craig, R.A., I. Katz, R.B. Montgomery and P.J. Rubenstein, "Meteorology of the Refract've Problem," Chap. 3 of Radiation Lab Series, Vol. 13, Propagation of Short Radio Waves, McGraw Hill, Edited by D.E. Kerr, 1951.

17. Johler, J.R., "Loran Radio Navigation Over Irregular, Inhomogeneous Ground With Effective Ground Impedance Maps," OT/Trer 22 (Suptd. of Doc., U.S. Gov. Print. Off., Washington, D.C. 20402), 1971.

18. Fredericks, R.J. M.W. Bird, K.A. Wheeler, "Recent Advances in Accurate Airborne Computation of Secondary Phase for Loran-C Radio-Navigation, " (Lear Stegler, Inc., Instrument Division, 4141 Eastern Avenue, S.E., Grand Rapids, Michigan 49508), 1975.

19. Johler, J.R., D.C. Hyovalti and W.B. Jones, "Impedance Maps to Predict the Effect of Irregular, Inhomogeneous Ground of Loran-C/D Radio Navigation Systems," OT Report 73-6 (Suptd. of Doc., U.S. Gov. Print. Off., Washington, D.C. 20402), 1973.

20. Fredericks, R.J., "A Simplified Algorithm for Improving the Absolute Accuracy of Loran-C Radio Navigation," Journal of ION, Winter 1974-1975, 1974.

21. Doherty, R.J. and J.R. Johler, "Interpretation of West Coast Loran-C Spatial Errors Using Programmable Calculator Analysis Techniques," 7th Annual Technical Symposium of the Wild Goose Association, 4 Townsend Road, Acton, Mass. 01720, 1978.

22. Johler, J.R. and R.H. Doherty, "Significance of Groundwave Propagation Anomalies Observed During a Loran-C Chain Validation," OT Technical Memorandum 76-22, (U.S. Dept. of Commerce, OT/ITS, 325 Broadway, Boulder, Colorado 80302), 1976.

23. Doherty, R.H. and J.R. Johler, "Calibration and Evaluation of the Unattended Ft. Hood, Texas Loran C/D Chain," OT Technical Memorandum 76-219 (U.S. Dept. of Commerce, OT/ITS, 325 Broadway, Boulder, Colorado 80302), 1976.

24. Pressy, B.G., G.E. Ashwell and C.S. Fowler, "The Measurement of the Phase Velocity of Ground-wave Propagation at Low Frequencies Over a Land Path," Proc. IEE 100, pt. III, 73-84, 1953.

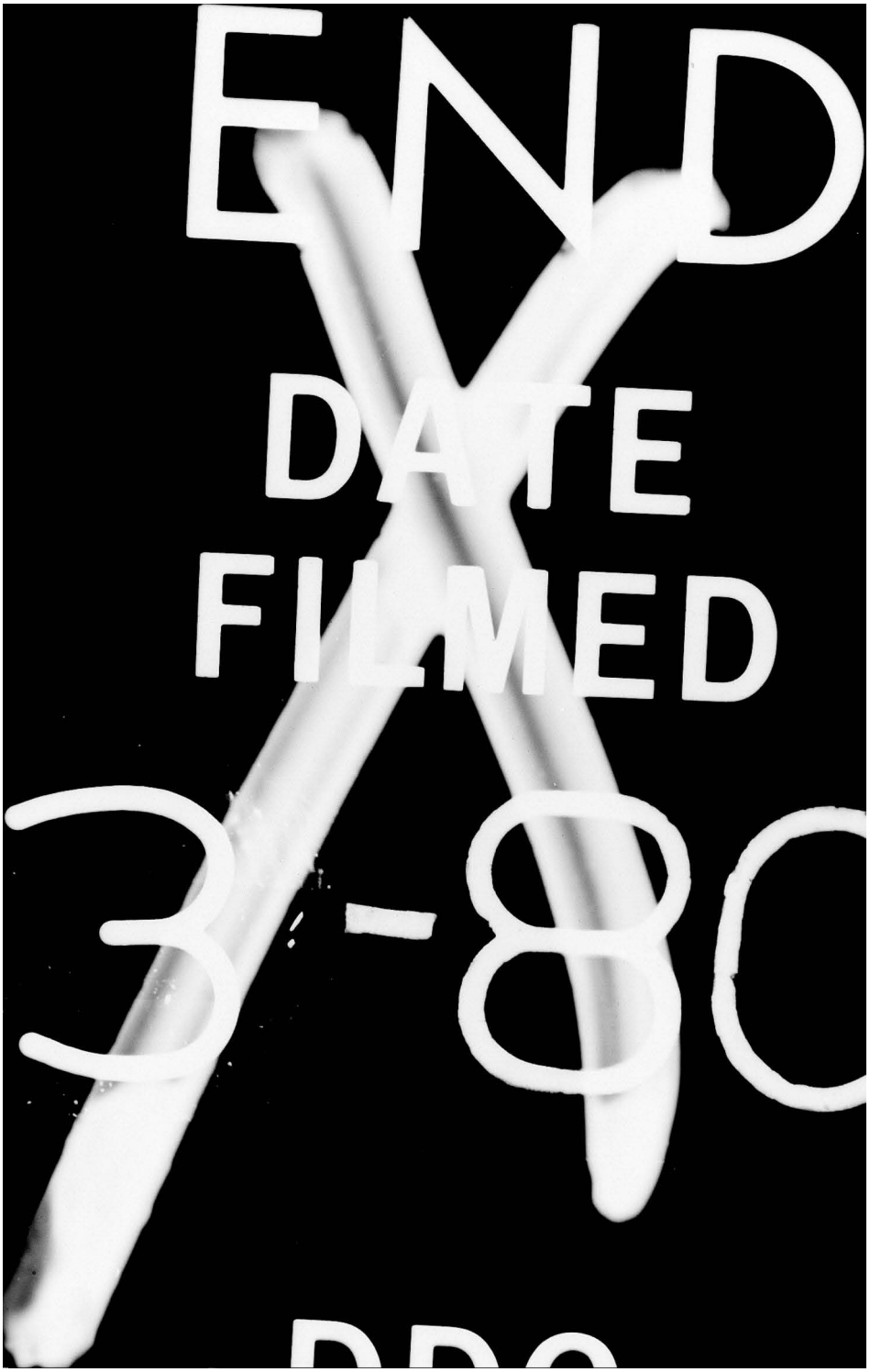
END
DATE
FILMED
3-80
DTIC

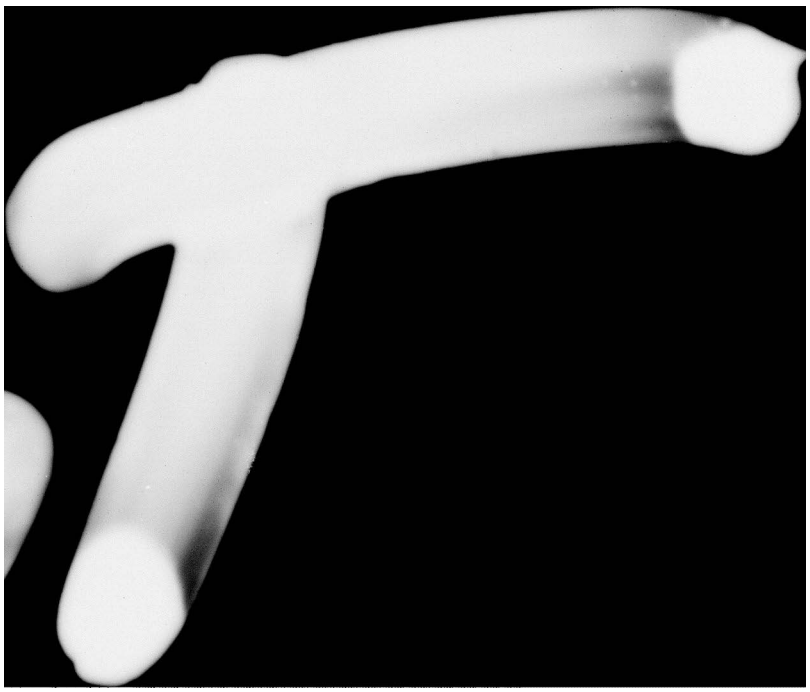

AD-A076 214 ANALYTICAL SYSTEMS ENGINEERING CORP BURLINGTON MA F/G 20/14
LORAN-C SYSTEM DYNAMIC MODEL: TEMPORAL PROPAGATION VARIATION ST--ETC(U)
JUL 79 L W CAMPBELL , R H DOHERTY DOT-CG-829358-A
UNCLASSIFIED ASECR-79-107 USCG-D57-79 NL

2 of 2
AD A 076214

END
DATE FILMED
7-80
DTIC


D A
076

SUPPLEMENTAR

INFORMATION

AD-A076214

Errata Sheet
for
Loran-C System Dynamic Model - Temporal Propagation Variation Study
Report No. DOT-CG-D57-79/NTIS AD-A076214

Page 4-1: Change to read as follows. Vertical indicators in margin denote where changes have been made. "and the phase changes associated with the surface refractive index is simply

$$\frac{\Delta \eta \cdot d,}{c}$$

which quantity is in microseconds if d is in kilometers and c in kilometers per microsecond. Therefore, a change from

$$\eta_a = 1.0002 \text{ to } 1.0004,$$

(the maximum η_a variation) over a propagation path with a length of 1000 km would yield a phase change of 0.67 microseconds. Normally the change in average value ($\eta_a = 1.000338$) over a day or during a weather change would be only 40 N-units (N-units = $(\eta_a - 1)\ 10^6$). Therefore, the maximum diurnal or weather change effect that could be attributed to changes in η_a for a 1000 km propagation path would be 0.133 microseconds, or 133 nanoseconds. This amount of variation may be nearly typical of the variations observed over a 1000 km propagation path during warm weather. However, in cold weather, the observed variations are considerably greater in magnitude than these values, reference (8). As a result the overall winter weather variations observed over an approximately 1000 km propagation path have been attributed to changes in the vertical lapse factor."

Page 3-7: After Eq. (5), change "h is in meters" to read "h is in 100 meters".

Page 6-3: Change Eq. for $\frac{dN}{dh}$ to read:

$$\frac{dN}{dh} = -\left[\frac{776 \times 1.268}{T} + \frac{77.6}{T^2}\left\{P + \frac{9620e}{T}\right\}\frac{dT}{dh} + \frac{77.6}{T}\left(1 - \frac{4810}{T}\right)\frac{de}{dh}\right]$$

Page 6-3: After Eq. for $\frac{dN}{dn}$, change "h = Height in meters" to read "h = Height in 100 meters."